DYNAMICAL SEASONAL PREDICTION AND PREDICTABILITY OF MONSOON

IN-SIK KANG

Climate Environment System Research Center, Seoul National University
Seoul, 151-742 Korea
kang@climate.snu.ac.kr

JAGADISH SHUKLA

Center for Ocean-Atmosphere-Land Studies
Calverton, MD, USA

Abstract

We present a historical review of the hypothesis of boundary forced predictability of monsoon, its limitations and the challenges in dynamical seasonal prediction of monsoon rainfall. We also present an assessment of the multi-model seasonal predictability of summer-mean precipitation over the Asian Monsoon-Western Pacific region by using 21 year (1979-1999) hindcast predictions of the five models, participating at the Asia-Pacific Economic Cooperation Climate Network (APCN). The five models consist of the current operational seasonal prediction models of NCEP, NASA, JMA, KMA, and SNU. The potential predictabilities of individual models are shown by various methods including the signal to noise ratio and anomaly correlations. Statistical methods for correcting the bias of the model prediction are developed and applied to individual model predictions. It is shown that the statistical correction is effective for enhancing the predictability, particularly for the Asian Monsoon – Pacific region, where the models have large bias. It is shown that a reasonably good seasonal prediction can be achieved when the multi-model predications are combined based on the composite of the individual predictions after applying the statistical correction to each separately.

Although this chapter describes mainly current status of the Tier-two seasonal prediction systems, the present skills of the Tier-one systems, utilizing coupled ocean-atmosphere models, are also examined using the data from Development of European Multimodel Ensemble System for Seasonal-Interannual Prediction (DEMETER). It is shown that the Tier-one system has advantage in producing better seasonal-mean anomalies, particularly in the western Pacific and Indian Ocean where air-sea interaction is active during summer. However, after applying a same correction method, it appears that the Tier one and Tier two systems produce a similar prediction skill.

1. Introduction

1) Historical Review

Variations of monsoon rainfall affect agriculture, drinking water, transportation, health, power, and the very livelihood of billions of people living in the monsoon region. It is no surprise therefore that for more than one hundred years several countries have tried to issue long range forecasts of monsoons (India Meteorological Department started issuing long range forecasts of monsoon rainfall in 1886). The operational long range forecasts of monsoon rainfall were based on empirical relationships derived from past observations of atmospheric pressure, temperature and wind. Blanford (1884) was the first one to suggest the use of a surface boundary condition (snowfall over Himalayas in the preceding winter) to predict the summer monsoon rainfall over India.

Charney and Shukla (1977, 1981) presented for the first time a conceptual hypothesis for monsoon predictability based on the influence of the boundary forcing at the Earth's surface. A brief historical perspective on this hypothesis is given here. Charney et al. (1977) had conducted AGCM experiments with NASA/GISS AGCM to investigate the influence of changes in albedo on rainfall over Sahel. In these experiments it was found that the summer rainfall variance among the three

ensemble members (each member was integrated only for 45 days) was quite small over the Indian monsoon region, indicating that the boundary conditions mainly control the Indian monsoon rainfall. In a symposium on monsoon dynamics in New Delhi in 1977, Charney reviewed some recent observational papers (Shukla and Misra (1977) for SST, Hahn and Shukla (1976) for snow cover), and a GCM experiment (Shukla (1975) for impact of Arabian sea SST).

Shukla and Misra (1977) had shown an empirical evidence of a possible relationship between Arabian sea surface temperature (SST) and Indian rainfall, and Shukla (1975) had shown that in the GFDL atmospheric general circulation model (AGCM), specification of (large) positive SST anomalies over the Arabian sea produced increase in monsoon rainfall over India. Hahn and Shukla (1976) revived the Blanford's hypothesis of snow–monsoon relationship by showing, using satellite derived snow cover data, an inverse relationship between the winter season snow cover over Eurasia and the subsequent summer monsoon rainfall over India. These results, combined with the results from the GISS model in which variance of seasonal rainfall among ensemble members was quite small, lead Charney and Shukla (1977, 1981) to propose a hypothesis that predictability of monsoon depends on the influence of boundary conditions at the earth's surface. The low variance among three ensemble members of the GISS model underestimated the role of internal dynamics in producing large intraseasonal and interannual variations of monsoon circulation and rainfall.

The Charney-Shukla hypothesis has been the central paradigm for monsoon predictability research during the past 25 years. However, no dynamical model has been successful, so far, in realizing the potential predictability of summer monsoon rainfall, especially over monsoon region. Whether our inability to capture the boundary forced signals is due to inadequate models and modeling strategies or due to intrinsic limits to the predictability of seasonal mean rainfall because of large natural intraseasonal variability of monsoon remains to be an open question and a topic of vigorous debate. In the following section we present a critical retrospective of the Charney-Shukla hypothesis and describe the barriers to realizing the potential predictability.

For the influence of the boundary conditions to be useful to predict monsoon rainfall, the following three conditions need to be satisfied: 1. There must be a large and persistent anomaly at the earth's surface, 2. There must be a well defined dynamical mechanism through which changes in the boundary condition will produce a corresponding change in seasonal mean monsoon rainfall, 3. The seasonal mean response (signal) must be sufficiently large and reproducible so that it can be distinguished from the intrinsic variability (noise) of the model due to internal dynamics alone. Large number of model simulations during the past decade with higher resolution AGCMs using advanced parameterizations have clearly shown that the internal variability over the monsoon region is much larger than that was shown by Charney and Shukla. This implies that large member ensembles are needed to distinguish the boundary forced response from internal dynamics variability. If the internal variability was at small spatial scales and at high frequency, large scale spatio-temporal averages (viz seasonal mean over whole India) could be predicted if the boundary forcings were indeed important, and if the models were able to simulate the appropriate physical effects.

The current generation of AGCMs have such large systematic errors in simulating both the mean and the variance of summer monsoon rainfall that it is not possible to conclude whether our current inability to make useful dynamical seasonal prediction is due to lack of boundary forced predictability or inadequacy of the current models and modeling strategies. However, recent research work in which model experiments are carried out with coupled ocean-atmosphere models suggests that the prescription of SST anomalies in AGCM experiments is an inadequate modeling strategy because SST anomalies in the Indian Ocean and the adjoining western Pacific Ocean are either forced by the atmosphere or evolve as a strongly coupled ocean-atmosphere process (Wang et al. 2004). If ocean-atmosphere coupling is indeed crucial for the Indian Ocean and western Pacific SST anomalies, predictability of monsoon must be investigated with coupled ocean-atmosphere models, which

currently have large systematic errors. The problem is further compounded by the fact that atmosphere-land interactions are also quite important for simulation and prediction of monsoon rainfall. Even if SST anomalies were able to force significant changes in large scale circulation, the local land-atmosphere interaction will modulate the ocean forced remote response and determine the actual changes in rainfall over land. Therefore, realistic models of the total climate system (ocean-land-atmosphere) are required to understand the predictability, and to make useful predictions of monsoon rainfall.

2) Challenges in Dynamical Seasonal Prediction of Monsoon

The current AGCMs and coupled models have been unsuccessful in producing skillful predictions of seasonal mean rainfall over monsoon region. Some of the major challenges are summarized below.

A. Simulation of monsoon climate: The Asian monsoon region has many unusual geographical features: very high mountains (Himalayas), the steep coastal regions of India (the western Ghats) and the Burmese coast, large number of islands in the maritime continent), which make it difficult to simulate the structure and variability of mean monsoon rainfall using coarse resolution models. While it is likely that very high resolution models will be able to simulate geographically forced structures of regional rainfall, the large discrepancy between the observed and the simulated rainfall, especially during the summer monsoon season, suggests some basic problems in the physical parameterizations, and especially the interactions between dynamics and moist convection. For example, nearly all AGCMs show incorrect simulation of summer mean rainfall over the Indian Ocean and the western Pacific (Kang et al. 2002b). The current models (both the AGCMs and the coupled models) also have large errors in simulating the structure and intensity of rainfall over land. It is unlikely that models with large errors in simulating the mean climate will be able to simulate and predict its interannual variability.

B. Simulation of interannual variability (modeling strategy): Inability of the current models to simulate the mean climate is perhaps the primary reason that the models are unable to simulate the interannual variability. It is therefore inevitable that these models will be unable to make a useful prediction of climate anomalies. In this paper it will be shown that the models indeed have large systematic errors in simulating the structure and magnitude of the monsoon climate anomalies. Whether the inability of the current models to simulate the observed rainfall and circulation anomalies is due to inadequate model resolution and physical parameterizations, or due to the incorrect modeling strategy of prescribing the SSTs has been addressed by several researchers. It has been shown by Wang et al. (2004) and Kirtman and Shukla (2002), that the coupled atmosphere-ocean processes are extremely important, and prescription of SST in the Indian Ocean and the western Pacific is a major factor in degrading the simulation of monsoon rainfall. Therefore an appropriate modeling strategy to estimate the predictability of monsoon and to make dynamical seasonal prediction will be to use coupled ocean-atmosphere models. However, the current coupled models need to be further improved to simulate the space-time structure of interannual variability of SST and rainfall.

C. Simulation of Intraseasonal Variability: There is a large body of observational and modeling research (Webster et al, 1998; Sperber et al, 2001) that clearly shows the importance of intraseasonal variations of rainfall both for understanding the predictability of seasonal mean rainfall and for societal applications. In particular, many studies indicate that the monsoon active and break phases are closely related to the Monsoon intraseasonal variations and the climatological rainy seasons in East Asia, such as Meiyu in China, Changma in Korea, and Baiu in Japan. Those rainy seasons appear to relate to phase locking of the intraseasonal variation to the climatological cycle (Kang et al. 1999) However, neither the current generation of AGCMs with prescribed SST nor the coupled ocean-atmosphere models are able to correctly simulate the intraseasonal variations (Wu et al. 2002; Waliser

et al. 2003). It is unclear whether this deficiency of models is due to inadequate resolution and parameterizations of moist convection, or due to inadequacy in simulating the coupled processes.

D. Land-atmosphere interactions: It is well known that even the remote effects of SST anomalies get strongly modulated by local atmosphere-land interactions, and therefore, the observed intraseasonal and interannual anomalies of rainfall over land are manifestations of coupled ocean-atmosphere-land interactions. The monsoon climate and its interannual variability is especially influenced by the three way interactions among ocean, atmosphere and land. This puts an additional challenge on climate models to simulate the mean monsoon circulation and its interannual variability.

E. Model dependent estimates of predictability: For a number of reasons, some of which are mentioned before, it is no surprise that the current generation of models give different estimates of SST forced "signal" and internal dynamics generated "noise," and therefore the estimates of seasonal and regional predictability (if defined as signal to noise ratio) are highly model dependent. In this respect, we are in the same situation today as Charney et al (1966) were about 40 years ago, when they found that the estimates of weather predictability were highly model dependent. It took more than 30 years before most of the NWP models of the world began to produce similar estimates of weather predictability. Likewise it is expected that as the climate models are improved to make more realistic simulation of observed climate and its variability, the estimates of seasonal predictability of monsoon will also improve.

3) Current Dynamical Seasonal Predictions

In spite of many challenges described above, dynamical seasonal predictions using general circulation models have been implemented by several operational centers in recent years. In particular, possible improvement of seasonal prediction has been sought by use of multi-model ensembles to remove the uncertainties associated with the spread of ensemble predictions with different initial conditions and the uncertainties associated with model parameterizations (Krishnamurti et al. 1999; Palmer et al. 2004). This chapter describes the present status of dynamical multi-model ensemble seasonal prediction system, particularly for the Monsoon precipitation.

In the ensemble simulation, all ensemble members are forced by the same SST but started from slightly different atmospheric initial conditions (Dix and Hunt 1995; Kumar and Hoerling 1995; Stern and Miyakoda 1995; Zwiers 1996; Kang et al. 2004). The basic idea of this approach is that the differences among the ensemble members can be used to quantify the noise due to internal dynamics, whereas the relative similarity between ensemble members can be considered as the atmospheric response to the external forcing. Thus, the ensemble mean (signal) can be considered as the component of the prediction forced by the SST, and the deviation from the ensemble mean as the stochastic internal component of the prediction. In this approach, the potential predictability is measured by the ratio between the externally forced SST signal and the internal noise using a standard statistical tool for this kind of problem: "analysis of variance" (ANOVA), which is detailed in many previous studies (Shukla 1981; Rowell et al. 1995; Rowell 1998).

Recently, attempts also have been made to reduce the uncertainty of models by simply compositing multi-model solutions (Kang et al. 2002a) and by using the so-called the "super-ensemble" method (Krishnamurti et al. 1999). The present skill of dynamical seasonal prediction is low, if any postprocessing is not applied. The poor skill is not only due to the atmospheric internal processes but also due to the model's inability in producing the atmospheric responses to external forcings, particularly the SST anomalies. This model bias in the external component arises from imperfect formulation and parameterization of various physical processes in the model. Different parameterizations produce different solutions. It may be assumed that the errors of those solutions are independent from each other, and various model solutions spread randomly but close to the observation. Then the composite of many model solutions can reduce the model random errors.

The model error can also be reduced by statistical correction methods. A major part of non-systematic error of each model can be corrected by a statistical relationship between the prediction and observed anomalies. Most commonly used methodology is the so-called coupled pattern technique (Graham et al 1994), based on singular value decomposition (SVD) analysis and canonical correlation analysis (CCA). Ward and Navarra (1997) applied SVD to simultaneous fields of GCM simulated precipitation and observed precipitation to correct the errors in the model response to SST forcing. CCA has been widely used for a statistical seasonal prediction system (Barnett and Preisendorfer 1987; Barnston 1994). A recent study by Feddersen et al. (1999) demonstrated that the postprocessed results are not sensitive to the choice among the methods based on the CCA, SVD, and EOF decompositions. In this paper, the postprocessing procedures of the error correction are developed based on the SVD analysis and a point-wise statistical downscaling method. By comparing the potential predictabilities with and without the correction, we can evaluate how the postprocessing of error correction enhances the predictability in the regions of interest.

At present, the dynamical seasonal prediction procedures are categorized as Tier-two and Tier-one systems. The Tier-two system treats the atmosphere and the ocean (specifically SST) separately. This system relies on an atmospheric GCM integrated with prescribed (either observed or predicted) SST boundary conditions and atmospheric initial conditions. The potential predictability of the Tier-two systems have been examined internationally by the Seasonal Model Intercomparison Project (SMIP II) initiated by the Climate Variability and Predictability Program (CLIVAR)/Working Group on Seasonal to Interannual Prediction (WGSIP). The purpose of SMIP II is to evaluate the current dynamical seasonal prediction systems in a framework, where the lower boundary conditions are prescribed with the observed SSTs for the 20 years 1979-98. On the other hand, SMIP/Historical Forecast Project (HFP) uses the predicted SST conditions instead of the observed, and therefore the SMIP/HFP evaluates the real seasonal predictability of current operational prediction systems.

The Tier-one system utilizes a coupled ocean-atmosphere model. At present, the climatology of coupled models has large systematic bias. However, as mentioned before, the coupled model has some advantage in simulating the monsoon anomalies particularly in the subtropical western Pacific and Indian Ocean, where air-sea interaction plays an important role in producing seasonal-mean anomalies. Recently, the European community has established the Development of European Multimodel Ensemble System for Seasonal-Interannual Prediction (DEMETER) based on the seven coupled models in European countries (Palmer et al. 2004). The aim of DEMETER is to develop a multi-model Tier-one seasonal prediction system and evaluate the skill of the prediction system. At present, ECMWF produces the seasonal prediction regularly based on the DEMETER. The present chapter shows the skill of the Tier-one DEMETER system and other Tier-two systems.

Section 2 describes the prediction experiment and the data utilized in the present chapter. The potential predictabilities of Tier-two systems are examined in terms of the signal to noise ratio in Section 3 and in terms of anomaly correlation in Section 4. The potential predictability is defined here as the predictability obtained by prescribing the observed (not predicted) SST boundary conditions in the model. Section 5 introduces a statistical correction method and shows how the prediction skill is improved after the correction. Section 6 shows the potential predictability of various multi-model ensemble prediction systems. In contrast to the potential predictability examined in the previous sections, the real predictabilities are assessed in Section 7 by using a Tier-two system with predicted SSTs and Tier-one systems (DEMETER coupled models). Summary and concluding remarks are given in Section 8.

2. Models and Experiments

The data utilized in the present study are obtained from the Asia-Pacific Economic Cooperation (APEC) Climate Network (APCN). The APCN is aimed at producing and disseminating a multi-model ensemble seasonal prediction based on operational prediction products of APEC member countries. Among them, used are the dynamical seasonal prediction data produced by Japan Meteorological Agency (JMA), Korea Meteorological Administration (KMA), National Aeronautical Space Agency (NASA), National Centers for Environment Prediction (NCEP), and Seoul National University (SNU), in part of the Seasonal Prediction Model Intercomparison Project (SMIP) II, leaded by the CLIVAR/Working Group of Seasonal to Interannual Prediction. The SMIP II extends the prediction target to two seasons for all four seasons (winter, spring, summer, autumn) of the 21 years of 1979-99, requiring each participating center to carry out more than 6 ensemble integrations for 7 months. The observed SSTs are prescribed for the integration. Therefore, the SMIP II can estimate the upper bound of seasonal predictability but not the actual predictability. See the details of SMIP II at the web page, http://www-pcmdi.llnl.gov/smip. The above models consist of different combination of physical parameterizations, listed and summarized in Table 1. The DEMETER data is also used in the present study. Details of the DEMETER can be found in Palmer et al. (2004) and the participating models of DEMETER are listed in Table 2.

The present study focuses on the predictability of seasonal-mean rainfall for boreal summer. For brevity, hereafter "boreal summer" is abbreviated to "summer". The prediction data of each model consists of 10 members of summer-mean precipitation for the 21 summers of 1979-99, except the NASA and JMA models of 9 and 6 members, respectively. The 10 members were generated with the observed initial conditions at 00Z and 12Z 27-31 May. The horizontal resolution of all data is converted to 2.5^{O} in longitude and 2.5^{O} in latitude. The observed precipitation data for the verification is obtained from the Climate Prediction Center Merged Analysis of Precipitation (CMAP) data set (Xie and Arkin, 1997).

3. Signal to Noise Ratio

The present section describes how well the AGCMs of the Tier-two system simulate the climatological summer-mean precipitation and its interannual variance. The variance is decomposed into the external (signal) part, related to the SST forcing, and the internal (noise) part, related to the atmospheric nonlinear internal dynamics, and the potentially predictable region is identified by examining the signal to noise ratio over the globe. Fig. 1a shows the observed climatological summer-mean precipitation for 21 years. Other figures in Fig. 1 show the simulated counterparts of Fig. 1a. The model climatology is obtained based on the average of 126 for JMA, 189 for NASA and 210 samples (10 members/each yr x 21 years). for other models, respectively. Although there are some differences, all models simulate the observed large-scale precipitation pattern, particularly large precipitations over the Bay of Bengal, surrounding regions of India, the western Pacific and ITCZ in the tropical central and eastern Pacific. A common failure of the models is the too much dryness over the equatorial eastern Indian Ocean. Also, the observed East Asian-western Pacific rainbelt is shifted to the inland region and Manchuria in all models except the JMA. This common shift of the model rainbelt was also demonstrated by the CLIVAR/AGCM Monsoon Intercomparison (Kang et al. 2002b).

The interannual variability of summer-mean precipitation is examined in terms of its variance. The anomaly is defined as the deviation of summer-mean precipitation from its climatology. Fig. 2a shows the variance of observed summer-mean precipitation for the 21 years. The spatial pattern of Fig. 2a is similar to that of Fig. 1a, indicating that large variability appears in the regions of large mean precipitation. Figs. 2b-2f are the corresponding variances of each model. Each model variance is estimated based on predictions of all members for the 21 years, and it will be referred to as the total variance. As in the observation, the spatial distribution of the simulated variance appears to be similar

to that of the corresponding climatological mean. But, the magnitudes of the simulated variances are quite different for different models. The NCEP variance is particularly large and about ten times larger than that of the JMA over Indochina, South China and Indian regions. The NCEP model has much larger interannual variances than the observed, and the JMA model has much less variances in most of the regions, particularly over the Asian monsoon region. The difference among the model variances is partly related to the difference in the mean climatology and to the different combination of model physics. But, it is difficult to identify which model physics is responsible for generating such large differences.

The total variance (σ^2_{TOT}) is divided into the external (σ^2_{SST}) and internal variances (σ^2_{INR}; Rowell, 1996). The ensemble mean is considered as the external component of the prediction forced by the SST forcing, and the deviation from the ensemble mean as the stochastic internal component of the prediction. The internal variance can be expressed as

$$\sigma^2_{INR} = \frac{1}{N(n-1)} \sum_{i=1}^{N} \sum_{j=1}^{n} (x_{ij} - \overline{x_i})^2 \qquad (1)$$

where x is the precipitation, i indicates the individual year, N=21, j is the ensemble member, and n=10. $\overline{x_i}$ is the ensemble mean. The external variance is obtained by the mean square of the deviation of each year's ensemble mean from the climatological mean and with a consideration of bias correction, as in Rowell (1996):

$$\sigma^2_{SST} = \sigma^2_{EN} - \frac{1}{n}\sigma^2_{INR}, \text{ and } \sigma^2_{EN} = \frac{1}{N-1} \sum_{i=1}^{N} (\overline{x_i} - \overline{\overline{x}})^2 \qquad (2)$$

where $\overline{\overline{x}}$ is the climatological mean, $\overline{\overline{x}} = 1/(Nn) \sum_{i=1}^{N} \sum_{j=1}^{n} x_{ij}$. It is noted that the sum of external and internal variances expressed above is equal to the total variance.

Figs. 3a-3e show the external variances of various models, and Figs. 3f-3j the internal variances. The signal to noise ratio, the ratio of the external part to the internal part of corresponding model, is shown in Figs. 3k-3o. All models produce large external variances over the tropical oceans, which are much larger than the internal variance of same model, particularly the ENSO region. Note that the JMA, NASA, and SNU models produce very little internal variances in the tropical Pacific. On the other hand, the NCEP model has large internal variability along the Pacific ITCZ region, although the external variances are still larger than the internal part over the region. This result indicates that the tropical rainfall is less controlled by the atmospheric internal processes and thus predictable for a given SST condition. In the extratropics, on the other hand, the internal variances are bigger than the external variances of the same model (Figs. 3k-3o), and therefore the extratropical atmosphere is more controlled by nonlinear stochastic processes and less predictable.

Over the Asian monsoon-western Pacific region, the external and internal parts appear to be equally important for all models, although some models (JMA, NASA, and SNU) have relatively large values of the signal to noise ratio over the region (Figs. 3k-3o) compared to those of the KMA and NCEP models. In contrast to other models, the KMA model produces relatively weak external variances but large internal variance over the western Pacific. As a result, the signal to noise ratio of the KMA model is small over the region, indicating less predictability for the Asian monsoon. It is interesting to note that the internal variance is generally proportional to the external variance. In particular, the large variance of the NCEP model shown in Fig. 2 is partly due to the large internal variance, particularly over the Asian Monsoon region. On the other hand, the internal variance of the JMA model is very weak. As a result, the JMA model has relatively large values of signal to noise ratio, although its forced variance is significantly weaker than those of the other models. It is also

noted that the internal variance is very much model dependent, indicating that the internal variations are not only controlled by the dynamics but also by model physics.

As shown in Fig. 3, the tropical rainfall variations are mainly controlled by the SST anomalies and therefore potentially predictable, if the model responses correctly to the prescribed SST. But, the model has systematic errors. Therefore, the signal to noise ratio shown in Figs. 3k-3o show the upper limit of predictability. The model error is estimated by the difference between the ensemble mean of model predictions and the corresponding observations. The error variances of each model are shown in Figs. 4a-4e. It is interesting to note that the spatial distributions of the errors for all models are similar. All models produce large systematic errors in the Asian Monsoon region and along the ITCZ. The ratio of the external variance to the error variance is shown in Fig. 4f-4j for individual models. If the ratio is bigger than one, the prediction signal can be considered to be larger than the error. Such regions appear in the central equatorial Pacific, the tropical Indian Ocean, and near the northeastern coast of South America. In other regions, particularly the Asian monsoon and western Pacific, all models produce errors which are bigger than the signals. This result indicates that although there exist large prediction signals in the monsoon region (Fig. 3), which are related to SST, the signals are poorly simulated by the models. In the remainder of this chapter, we investigate whether it is possible to make a reliable monsoon prediction, if the systematic errors were corrected. The error correction will be discussed in Section 5.

4. Potential Predictability of Various Models

The prediction skill of each model is measured by using the correlation between the ensemble-mean predictions and the observations for 21 years. Since the observed SST was prescribed in the hindcast predictions, this prediction skill is a measure of potential predictability. In contrast, the real predictability should be measured based on the hindcasts with predicted SST and will be shown in Section 8. Fig. 5 shows global distribution of correlation coefficient between the observed and predicted ensemble-mean precipitation at each grid point for the 21 summers. The correlations of various models are shown in Figs. 5b-5f, and Fig. 5a shows the correlations between the observation and the five model composite. As expected in the previous section, all models have large correlation over the ENSO region, where the external (forced) variance exceeds the internal variance and the model systematic error. In contrast, over the Monsoon region, the correlation skill is very poor for all models. It is noted that the model composite does not help to improve the correlation skill. In the subtropical western Pacific and the Atlantic Ocean, all models and the composite have large negative correlation values. The negative correlation in the western Pacific is due to model bias, where the external response has large systematic errors (Fig. 4). Recently, Wang et al. (2004) suggested that the poor simulations of precipitation over the western Pacific is due to the two-tier prediction system, where the atmosphere is forced by the prescribed SST. This provides an additional evidence that the ocean-atmosphere coupled processes are important for the summer precipitation anomalies in the western Pacific.

The spatial correlation over the globe between the ensemble mean seasonal prediction and the corresponding observed precipitation at each year is shown in Fig. 6a. Correlation values of various models are marked with the symbols shown at the bottom of the figure, and those of the model composite with a line. The figure shows that none of the models have a predominant performance to the others, however, the model composite has a best skill with exceptions of few years. The composite correlation skill varies from about 0.2 in early 1980s to 0.66 for 1987. It is noted that the relatively large correlation skill appear in the years of ENSO, particularly for the El Nino summers of 1987, 91, 97, and the La Nina summers of 1988. It is also noticed that the correlation skill of 1983 summer is relatively high, although the tropical Pacific SST was normal.

The spatial correlations of the Monsoon region (40°-160°E, 20° S-30° N) are also computed for the five models and the model composite, and their year to year variations are shown in Fig. 6b. With a few exceptions, all models poorly predict the monsoon precipitation for most of the summers. The model composite shows the correlation values below 0.3 for most of the summers, except the years of 1981, 86 and 87. Among those years, only one summer (1987) was a El Nino year. To examine the SST impact on the monsoon prediction, the SSTs are composed for the four years of good prediction cases (1981, 86, 87, 90) and for the years of bad prediction cases (1980, 82, 94, 97), and the composite SST anomalies are shown in Fig. 7. Comparison between Figure 7a and 7b clearly demonstrate that the monsoon precipitation is indeed closely related to the SST anomalies, particularly over the oceans surrounding the Asian monsoon region and the eastern tropical Pacific.

We also examine the prediction skill of a hypothetical perfect model (a model with no systematic error). The correlation skill of the perfect model is estimated for each model by considering one of the ensemble members as observation, and that is correlated with the ensemble-mean of the other members. Fig. 9a shows the global pattern correlations for various perfect models. Different perfect models have different correlation skills, which are proportional to the ratio of the external variability to the internal variability shown in Fig. 3. As expected from Figures 3k-3o, the perfect model configurations of JMA, NASA, and SNU have higher correlation skills (the average global pattern correlation about 0.8) than those of KMA and NCEP. For the monsoon region (Fig. 8b), the perfect model correlation values highly depend on the model. Fig. 8b shows that the NASA and KMA models, respectively, have highest perfect model correlations (the average value of about 0.7) and lowest correlations (the average value of about 0.3). It is noted that these perfect model correlations are the upper-limit of predictability that the models can have, if the real climate variability is same as that of model, and that represent the degree of reproducibility of each model.

5. Prediction Skill after Error Correction

(1) Error Correction and Verification Methods

The model bias in the external component appears in a systematic way in both the climatological mean and the anomaly component. The mean bias can be corrected by subtracting the prediction climatology from the prediction of each individual year. The systematic error of the anomaly component is related to incorrect performance of GCM in simulating the anomalies, predominantly forced by the SST anomalies. It is noted that a slight shift of the spatial pattern of model anomaly can result in a substantial drop in skill scores when the skill is measured based on the performance at individual grid-points. Here two statistical correction methods are introduced. The first method is based on the singular value decomposition (SVD) (Ward and Navara 1997; Feddersen et. al. 1999; and Kang et al. 2004). As in Kang et al. (2004), the systematic errors of the predicted anomaly are corrected by replacing the SVD modes of prediction to the corresponding observed modes. The transfer function for the replacement can be constructed as follows,

$$X(x,t) = \sum_{i=1}^{P} \alpha_i Y_i(t) R_i(x) \qquad (3)$$

where, X(x,t) is the corrected field, Y(t) is the time coefficients of the SVD mode for the predicted field, and R(x) is the projection of SVD singular vector onto the observed field. *i* is the mode number, P the total number of the SVD modes, and α is the correlation coefficient between the time series of the SVD mode of prediction and the corresponding SVD time series of observation. It is noted that before obtaining the SVD modes, the EOF analysis is applied to the predicted and observed anomalies, separately, and the observed and predicted fields are reconstructed by retaining the leading

10 EOF modes of each field. This process filters out small scale anomalies and smoothes the spatial fields.

It is noted that the SVD based correction method is working well in the region where the principal eigenmodes are distinctive. However, this method can not correct the bias which is not related to a leading SVD mode and/or has a local character. Another correction method, used in this chapter, is the so-called "Coupled Pattern Project Method (CPPM)," which is based on the large-scale patterns of model variables correlated to a local (grid) observed precipitation. Once, the model patterns are determined from hindcast prediction data, the local precipitation can be predicted by a linear combination of the predictors obtained by projecting the patterns to the dynamical prediction data. Thus the CPPM can be considered as a statistical downscaling method for a local prediction. Here, it is important to define optimally the domains of the patterns for each local prediction, which are predetermined based on hindcast prediction data. The optimum domains are obtained by repeatedly comparing the prediction skill of the corrected prediction by changing and moving the domains over the globe. The domain sizes scanned are from 30^o longitude x 20^o latitude (minimum size) to 120^olongitude x 50^o latitude (maximum size). In the scanning procedure, the domains are selected only if the statistical significance of a grid point in the domain exceeds a certain threshold value, 95% significance level. Here, the variables used as predictors are precipitation and 850hPa temperature. As shown later, the CPPM is a powerful method that can be used for all grid points of the model.

Double cross validation (Kaas et al. 1996) is used to evaluate the skill of the bias-corrected prediction anomalies. The relatively short period of record, 21 years, utilized in the present study may overestimate skill scores by overfitting random variability as indicated by Davis (1976). To control this problem, the correction method developed without the target year is applied to the year. In addition, in each step of cross-validation procedure, cross-validated expansion coefficients of the SVD modes are computed in order to select the modes being included in the bias correction. Details of the present verification procedure can be found in Feddersen et al. (1999) and Kang et al. (2004). For the CPPM, the patterns used for the whole period of prediction are determined optimally based on a double-cross validation procedure.

It is noted that the corrections of prediction toward observation based on both the SVD and CPPM leads to loss of variability in absolute magnitude; that is, the corrected field stays close to climatology. Thus, it may be necessary to apply some sort of inflation method to the adjusted field. The most common way of inflation is to multiply the adjusted values by the ratio between the standard deviation of the observations and that of the adjusted values. In the present study, the inflation factor is obtained by combining the common way of inflation and the weighting factor considered by Feddersen et al. (1999). The weighting factor depends on the magnitude of local variability of adjusted field. This approach leaves grid points of small variability, which usually have little skill, uninflated, while concentrating the inflation on more skillful grid points with large variability. The inflation factor IF_k in a grid point k is defined here as,

$$IF_k = \frac{\sigma_{k,obs}}{\sigma_{k,fct}} w(\sigma_{k,fct} / \sigma_{\max,fct}) \qquad (4)$$

where $\sigma_{k,obs}$ is the standard deviation of observation, $\sigma_{k,fct}$ is that of the bias-corrected simulation anomaly, $\sigma_{\max,fct}$ is the maximum value of $\sigma_{k,fct}$, and $w(x)$ is an s-shaped weight function $w(x) = \{1 + \tanh[6.9(x - 0.5)]\}/2$ which is close to zero for x=0 and close to one for x=1.

(2) Predictability after Error Correction

The error correction method introduced above is applied to the SNU predictions here and the applicability of the method to the seasonal prediction is examined based on the one model result. It is then applied to the other model predictions in the next section. Before making the correction, we examined how well the SNU model reproduces the EOF modes of precipitation variability over the globe. Figure 9a shows the first eigenvector of observed summer mean precipitation which explains 24.3% of total variance, and Fig. 9c is the predicted counterpart explaining 39.0% of total variance. Both figures are characterized by the east-west seesaw pattern between the anomalies in the tropical central Pacific and Indonesian subcontinent, although the model centers are shifted to the east. Other noticeable differences include sign differences in the subtropical western Pacific and the Indian Ocean eastward from 60E. The poor performance of the model in those regions is already mentioned in the previous section. The time series associated with the eigenvectors, shown in Fig. 9e, vary in a similar way and are related to ENSO SST anomalies. The difference between the model and observed eigenvectors in the subtropical western Pacific and Indian Ocean is due to failure of the model to simulate the responses of ENSO SST anomalies.

The second eigenvector of the observed summer-mean precipitation shown in Fig. 9b explains 15.7% of total variance. The spatial pattern is characterized by large variations in the subtropical western Pacific. The model counterpart, shown in Fig. 9d, shows that the model reproduces the western Pacific center but with much weaker amplitude. It also produces anomalies in other regions in the Pacific and Indian Ocean that are somewhat different from the observations. However, the similarity between the time series associated with observed EOF modes and the corresponding time series of predicted modes provides hope of error correction for the predicted field. The error correction has been done by using eq. (3) and the SVD modes, which represent more clearly the coupled modes of observed and predicted fields than the EOF modes do. The two leading SVD singular vectors (not shown) are very similar to the corresponding EOF eigenvectors shown in Fig. 9. The similarity can be expected from Figs. 9e and 9f, where the two time series of the observed and predicted modes vary almost simultaneously, indicating that the two EOF modes are coupled to each other. The first four SVD modes are used for the correction. The fifth and higher modes consist of small scale patterns and explain small fraction of the variance. Sum of the four modes explains 41.2% of the total variance.

Fig. 10a shows the spatial distribution of the correlation coefficient between observations and the corrected seasonal predictions based on the SVD method. Double cross validation procedure is applied to obtain the correlation skill. The correlation coefficients of corrected prediction are replaced by those without correction, if the former is smaller than the latter. Those locations are in the central tropical Pacific, where the correlation coefficient of the original prediction (Fig. 3) is already very large. Clearly, in most of the regions, the predictability is much enhanced by the statistical correction. The enhancement of predictability is particularly pronounced in the western Pacific where the correction skill is negative without correction (Fig. 5f) but has relatively large positive values after correction. The correlation skill of the corrected prediction based on CPPM is shown in Fig. 10b. In the tropics, both correction methods produce similar results. In the subtropics and extratropics, however, the CPPM has a superior ability in correcting the errors, particularly in the western Pacific.

The prediction skill of monsoon precipitation is shown in Fig. 11 in terms of the spatial pattern correlation between the observed and predicted fields of each year for the monsoon domain of 10^{O}N-40^{O}N and 80-160^{O}E. In the figure, the open bar indicates the pattern correlations without correction, and the shaded and black bars indicate those with the corrections based on the SVD and CPPM, respectively. The predictability is much enhanced by the corrections for most of the years. In particular, for the years such as 1980, 1985, 1987-1989, and 1991, the spatial correlations with

negative values before correction have relatively large positive values after corrections. In the years 1995 and 1996, on the other hand, the skill is degraded by the corrections. The 21-year averages of correlation values are 0.05, 0.24, and 0.32 for the predictions without correction and with the SVD and CPPM correction methods, respectively. Since the CPPM has a better performance than the SVD method, hereafter all corrections are made based on the CPPM method.

6. Multi-model Potential Predictability

The use of multi-model ensemble prediction for better seasonal prediction accounts for the following scientific reasons. Whilst the seasonal prediction is an initial-value problem and hence is sensitive to errors in initial conditions, a limitation on the skill of such predictions also arises from uncertainties in the representation of the basic equations that govern climate, particularly in the parameterization of unresolved processes (such as cloud formation and dissipation). To account for uncertainty in model formulation, ensemble members can be run with different sets of model formulations, each consistent with the full untruncated equations of climate. This can be achieved by generating the ensemble members from a set of quasi-independent state-of-the art climate models. By running several models each from multiple initial conditions, a multi-initial-condition and multi-physics-model ensemble forecast can be constructed.

There are several ways of combining the multi-model outputs. A most simple way is a composite. After Krishnamurti et al. (1999, 2000), scientists have tried to improve weather and climate forecasts using an approach called the multi-model "superensemble." The skill of superensemble method depends strongly on the post-processing algorithm for the multiple regression of multi model solutions toward observed fields during a training period. For the post-processing, the respective weights for individual models are generated using a multiple regression technique. The conventional superensemble forecast (Krishnamurti et al., 2000) can be constructed by the following formula.

$$S = \overline{O} + \sum_{i=1}^{N} a_i (F_i - \overline{F}_i)$$

Where, F_i is the i^{th} model forecast, $\overline{F}_i$ is the mean of the i^{th} forecast over the training period, $\overline{O}$ is the observed mean over the training period, a_i is the weighting factor of i^{th} model, and N is the number of forecast models involved. The design of an optimal weighting function for a long-term forecast is a key for the development of multi-model superensemble system. There are four different methods in computing the weight factors; a conventional linear multi-regression (Krishnamurti et al. 1999,2000), the Gauss-Jordon method, the Singular Vector Decomposition (SVD) method (Yun et al. 2003), a neural network method.

In the present section, the multi-model predictions are combined by the three methods: a simple composite (MME1), the superensemble based on SVD (MME2), and the composite of model predictions after each model prediction corrected by the statistical CPPM method (MME3). It is mentioned that the superensemble method is also applied to the predictions after error correction However, the superensemble in this case dose not provide a better skill compared to the composite of the corrected predictions. It may be because of double fitting to the observation: the first fit of the prediction to the observation for the correction and the second fit for the superensemble.

The spatial pattern correlations over the monsoon region for 1979-99 are obtained by using MME1, MME2, and MME3, and those are plotted in Fig. 12. As shown in Fig. 6b, the composite is not always better than the best individual model prediction, but the average skill of the composite is comparable to that of best individual model. Therefore, the choice of composite prediction will be generally safe since we do not know the best model for the prediction. On the other hand, the

superensemble skill (MME2) appears to be always better than that of best individual model with a few exception. But, as shown in the previous section, the prediction skill of individual model after error correction is usually much better than that of the raw prediction. The correlation skill of MME2 appears to be comparable to that of the best individual model after correction. The composite of corrected predictions (MME3) has usually a superior correlation skill than any of the corrected individual models. In most years, the MME3 produces best correlation skills among the multi-model ensemble methods. The MME3, which is the best system among the prediction systems used here, produces the 21 year average correlation skill of 0.54 for the monsoon summer prediction, which has a statistical significance. The correlation skills in other regions and other seasons should be different, and their usefulness should be examined separately. In conclusion, the dynamical monsoon seasonal prediction requires a multi-model system with sophisticated correction methods, which need further research efforts.

7. Real Seasonal Predictability

In the previous sections, the seasonal predictability was investigated by using the hindcast predictions with observed SST condition. However, a real operational prediction should use predicted SST as a boundary condition of model integration. The methods of SST prediction currently being used are a persistence, various kinds of ocean-atmosphere coupled model, and various statistical models. In the present chapter, the SST prediction was made by using a combination of the intermediate coupled model (Kang and Kug 2000) mainly in the tropical Pacific between 20^{o}S and 20^{o}N, statistical models for extratropical oceans and Indian Ocean, and a persistence of anomalies in the region where the persistence gives the best skill. The prediction method of Indian Ocean SST can be found in Kug et al. (2004).

By prescribing the predicted SSTs as a boundary condition, the 10 members of SNU atmospheric GCM integrations were performed using the 10 NCEP initial conditions of 12 hr interval for the period from 00Z 26 April to 12Z 30 April. Except the SST boundary condition, the prediction experiment is exactly same as that of the SMIP II described in Section 2. The monthly mean SSTs from April to August are predicted, and the daily SST data prescribed in the AGCM are obtained by linear interpolation of the monthly means. The present experiment is a part of Seasonal Model Intercomparison Project/Historical Forecast Project (SMIP/HFP) initiated by CLIVAR/WGSIP. Since the SMIP/HFP historical prediction data is only available for the SNU model at present, the real predictability is examined only for the SNU model.

Fig. 13 shows the distribution of correlation coefficient between the observed and predicted monthly-mean SST anomalies for the 21 years. The correlation skill at each grid point is calculated based on a cross validation method. The correlation skill of May (the second month of the prediction) is relatively high in most of the regions, except in the Gulf Stream region. From June to August, the correlation skill is reduced with time, particularly over the extratropical Pacific between 20^{o}N and 40^{o}N. Over the tropical region, on the other hand, the high correlation skill is almost maintained until August. The skill is particularly high (the values larger than 0.7) in the ENSO region and the tropical Indian ocean. It is interesting to note that the correlation in the tropical western Pacific has a minimum value in June and becomes increased in July and August.

The correlation skill of the real seasonal-mean prediction is measured in terms of the spatial correlation coefficient over the globe. Fig. 14 compares the correlation skills of the SMIP (open bar), predictions with observed SST, and the SMIP/HFP (shaded bar), predictions with predicted SST. As expected, the correlation skill of SMIP/HFP at each year (the 21 year average correlation value of 0.25) somewhat lower than that of SMIP (the average value of 0.34) with a few exceptions. After the statistical correction introduced in Section 5, the correlation skill of the real prediction (solid line) is

much improved and its averaged correlation value for 21 years becomes 0.48. Interestingly, the correlation skill of the corrected SMIP/HFP is similar to that of the corrected SMIP (shaded line, the 21 year averaged value of 0.43) for most of the years. At present, the reason is not clear but may be due to the fact that the level of uncertainty in fitting to the observation (correction) can be comparable to the loss of correlation skill by predicting SST. The results should be further examined with many other prediction models.

As mentioned in Introduction, most operational centers use the Tier-two system, but the European groups have constructed a Tier-one multi-model seasonal prediction system, DEMETER, utilizing seven ocean-atmosphere coupled models in the European countries, listed in Table 2. Here, we examine the prediction skill of the DEMETER system. Fig. 15 shows the correlation skills of summer-mean SST for the individual models and the multi-model ensemble over the globe. All models have relatively high correlation skill over the tropical Pacific and relatively low in the extratropical oceans. The correlation skill of the multi-model composite, shown in Fig. 15a, is higher than those of individual models in most of regions and particularly high (over 0.8) in the tropical Pacific. Those individual correlation skills shown in Fig. 15 can be compared to that of the SST prediction of the SNU Tier-two system shown in Fig. 15i. The SST prediction skill of the Tier-two system is comparable to or a bit higher than those of the DEMETER coupled models in most of the regions.

The prediction skills of precipitation of the coupled models, shown in Fig. 16, are relatively high in the tropical Pacific but poor in other regions. The skill of the multi-model composite (Fig. 16a) is similar to that of the best model. Comparison of individual Tier-one systems to the SNU Tier-two HFP system (Fig. 16i) indicates that the Tier-one system appears to be better than the Tier-two system, even though both the Tier-one and Tier-two SST predictions are comparable to each other. However, this comparison can not be generalized at present because only one Tier-two system is compared to many Tier-one systems. The better prediction of precipitation of the coupled model is distinctive in the western Pacific, where the Tier-two system produces negative correlation skills, indicating that the seasonal-mean atmospheric state does not passively respond to the SST but is determined by ocean-atmosphere interaction processes in the western Pacific.

The year-to-year variations of spatial pattern correlation for the 60^{o}S-60^{o}N domain between the predicted and observed precipitation are shown in Fig. 17. Shaded and dark circles indicate the correlation values of raw and corrected predictions, respectively. The average values of the seven models at each year are connected by the shaded line (raw prediction) and the dark line (corrected prediction). These averaged values can be compared to the corresponding values of the SNU Tier-2 HFP prediction. For the raw prediction case, the average performance of the Tier-one systems (the 20 year average value of 0.33) is better than that of the Tier-two system shown by the shaded bar in Fig. 14 (the 21 year average of 0.25). On the other hand, the average performance of corrected Tier-one systems (20 year average value of dark line, 0.46) is similar to that of the corrected Tier-two system, shown in Fig. 14. These results indicate that the two systems with a same correction may produce similar results. However, further researches are needed with same numbers of Tier-one and Tier-two systems to make more conclusive statements.

The MME3 multi-model ensemble method (composite of the corrected predictions), previously shown as the best among several multi-model ensemble methods treated in this Chapter, is now applied to the DEMETER predictions. The solid line in Fig. 18 shows year-to-year variations of the spatial pattern correlation between the observed and the MME3 precipitations for the region between 60^{o}S and 60^{o}N. The 20 year averaged value of the correlation values of the DEMETER MME3 is 0.58, which is somewhat lower than the value (0.62) of the multi-model composite of five corrected Tier-two predictions with observed (not predicted) SST condition (SMIP II), shown in Section 6. But those two correlation values are within a same significance level. Although the multi-model Tier-2

system with predicted SST can not be compared to the multi-model Tier-1 system at present, it may be assumed that the two systems may produce a similar prediction skill. This assumption is based on the results of Fig. 14 that the Tier-2 systems (with observed and predicted SST) with a same correction produce a similar prediction skill. However, this statement again deserves a further research. Fig. 18 also shows the correction skill of DEMETER MME3 for the Monsoon region (shaded dashed line). The 20 year averaged of the correlation values is 0.56. Interestingly is that the interannual variation of the Monsoon prediction skill is similar to that of global prediction skill. It is due to the facts that the global and monsoon prediction skills largely depend on the tropical Pacific SST related to ENSO.

8. Summary and Concluding Remarks

The present chapter showed present status of state-of-the-art dynamical seasonal prediction systems and demonstrated possible improvement of the predictions based on statistical correction and combination of several independent predictions. In particular, seasonal predictability of summer-mean precipitation over the Asian Monsoon-Western Pacific region is assessed by using 21 year hindcast predictions of five models for 1979-1999. The five models consist of the operation seasonal prediction models of Japan Meteorological Agency (JMA), Korea Meteorological Administration (KMA), National Aeronautical Space Agency (NASA), National Centers for Environment Prediction (NCEP), and Seoul National University (SNU). The historical prediction data were produced as part of CLIVAR/Seasonal Prediction Model Intercomparison Project II (SMIP II). In this experiment, the SST boundary conditions during the prediction are prescribed with observed SSTs, and thus the potential predictability has been assessed. The potential predictabilities of individual models and a multi-model ensemble system are shown by various methods including the signal to noise ratio based on the analysis of variance and the anomaly correlations. In addition to the potential predictability, the real predictability of seasonal mean precipitation of the Tier-two and Tier-one systems, have been assessed, respectively, based on the SMIP/HFP experiment, where the SSTs for the prediction period are predicted, and based on the coupled model predictions from the DEMETER project.

The signal to noise ratio of seasonal mean precipitation over the monsoon region is lower than those of other tropical regions. In addition to large noise, all Tier-two models produce large systematic errors in the Asian Monsoon region, particularly in the western Pacific. As a result, all models produce very poor correlation skill over the Monsoon region. The model composite prediction does not help to improve the correlation skill. For the subtropical western Pacific and the Atlantic Ocean, all models and the composite show the correlation skills with relatively large negative values. The negative skill in the western Pacific is due to model bias, where the external response has a large systematic error. Recently, Wang et al. (2004) suggested that the poor simulations of precipitation over the western Pacific is due to the two-tier prediction system, where the atmosphere is forced by the prescribed SST, but in nature the ocean-atmosphere coupled processes are active and atmospheric feedback to the ocean, which is missing in the two-tier approach, is important in the western Pacific.

To correct the model bias, statistical methods based on singular value decomposition (SVD) and a coupled patter project method (CPPM) were developed and applied to individual model predictions. It is shown that the statistical correction is effective in enhancing the predictability, particularly for the Asian Monsoon–Pacific region, where the large model bias is included in the leading eigenmodes of forced signal (Kang et al. 2004). The enhancement of predictability is particularly pronounced in the western Pacific where the correction skill is negative without correction but has relatively large positive values after correction. It is shown that the point-wise correction using the CPPM is generally better than the correction with leading SVD modes. Seasonal predictability of multi-model ensemble prediction is also assessed by using several multi-model methods including simple composite, various super-ensemble techniques and a composite of corrected individual predictions. It is shown that a reasonably good dynamical seasonal prediction can be achieved when the multi-model predications

are combined based on the composite of the individual predictions after applying the statistical correction.

The multi-model seasonal prediction based on coupled models is also examined by using the hindcast prediction data of DEMETER, which is an international European project where nine European coupled models have participated (Palmer et al. 2004). It has been anticipated that the Tier-one system often produces large systematic errors, particularly in the extratropical region, compared to those of the Tier-two system with the prescribed SST anomalies obtained from the same Tier-one system. However, this study shows that the Tier-one system can better predict the summer-mean precipitation particularly over the Monsoon-western Pacific region, where the ocean-atmosphere feedback is active. Although the DEMETER Tier-one systems generally produce better prediction skills over the globe compared to a Tier-two system with predicted SST, the two systems produce a similar prediction skill after statistical correction. The spatial correlation skill of the DEMETER MME3 for summer-mean precipitation, the best among the multi-model ensemble systems treated in the Chapter, is 0.58 over the globe and 0.56 over the monsoon region. These values may represent the summer-mean precipitation prediction skills that we can achieve with dynamical prediction models at present.

Acknowledgments

The authors appreciate the SNU colleagues and students, Dr. Jong-Sung Kug, Ms. Kyung Jin, Mrs. Jin Ho Yoo, Doo-Young Lee, and Ho-Yong Jeong, and Dr. June-Yi Lee at NASA/GSFC, who contributed their works to the materials presented in this Chapter. The present study was supported by the Climate Environment System Research Center at Seoul National University and the Korea Meteorological Administration.

References

Barnett, T. P., and R. Preisendorfer, 1987: Origins and levels of monthly and seasonal forecast skill for United States surface air temperatures determined by canonical correlation analysis. *Mon. Wea. Rev*., **115**, 1825-1850.

Barnston, 1994: Linear statistical short-term climate predictive skill in the Northern Hemisphere. *J. Climate*, **7**, 1513-1564.

Blanford, H. F., 1884: On the connection of the Himalaya snowfall with dry winds and seasons of droughts in India. *Proc. Roy. Soc*. London. **37**, 3.

Bonan, G.B., 1995: Land-atmospheric interactions for climate system models: Coupling biophysical, biogeochemical and ecosystem dynamical processes. *Remote Sensing of Environment*, **51**, 57-73.

Charney, J. G., R. G. Fleagle, H. Riehl, V. E. Lally, and D. Q. Wark, 1966: The feasibility of a global observation and analysis experiment. *Bull. Meteorol. Soc.*, **47**, 200-220..

_____, W. J. Quirk, S.-H. Chow, and J. Kornfield, 1977: A Comparative Study of the Effects of Albedo Change on Drought in Semi–Arid Regions. . *J. Atmos. Sci*., **34**, 1366–1385.

_____, and J. Shukla, 1981: Predictability of monsoons. Paper presented at the Monsoon Symposium in New Delhi, India, 1977, and published in the book *Monsoon Dynamics*, Eds., Sir James Lighthill and R. P. Pearce, Cambridge University Press, pp. 99-110.

Davis, R. E., 1976: Predictability of sea surface temperature and sea level pressure anomalies over the North Pacific Ocean. *J.Phys. Oceanogr*., **6**, 249-266

Dix, M. R., and B. G. Hunt, 1995: Chaotic influences and the problem of deterministic seasonal predictions. *Int. J. Climatol*., **15**, 159-164.

Feddersen, H., A. Navarra, and M. N. Ward, 1999: Reduction of model systematic error by statistical correction for dynamical seasonal prediction. *J. Climate*, **12,** 1974-1989.

Graham, N. E., P. Barnett, R. Wilde, M. Ponater, and S. Schubert, 1994: On the roles of tropical and midlatitude SSTs in forcing interannual to interdecadal variability in the winter Northern Hemisphere circulation. *J.*

Climate, **7**, 1416-1441.

Hahn, D. and J. Shukla, 1976: An apparent relationship between Eurasia snow cover and Indian monsoon rainfall. *J. Atmos. Sci.*, **33**, 2461-2436.

Holtslag, A.A.M., Boville, B.A.. 1993: Local Versus Nonlocal Boundary-Layer Diffusion in a Global Climate Model. *J. Clim*. **6**, 1825–1842.

Hong, S.-Y., and H.-L. Pan 1996: Nonlocal Boundary Layer Vertical Diffusion in a Medium-Range Forecast Model. *Mon. Wea. Rev.* **124**, 2322–2339.

Kaas, E., T.-S. Li, and T. Schmith, 1996: Statistical hindcast of wind climatology in the North Atlantic and northwestern European region. *Climate Res.,* **7**, 97-110.

Kang, I.-S., C.-H, Ho, Y.-K, Lim, K.-M. Lau. 1999: Principal Modes of Climatological Seasonal and Intraseasonal Variations of the Asian Summer Monsoon. *Mon. Wea. Rev*, **127**, 322–340.

_____, K. Jin, B. Wang, K.-M. Lau, J. Shukla, V. Krishnamurthy, S. D. Schubert, D. E. Waliser, W. F. Stern, A. Kitoh, G. A. Meeh, M. Kanamitsu, V. Y. Galin, V. Satyan, C.-K. Park, and Y. Liu, 2002a: Intercomparison of the Climatological variations of Asian summer monsoon precipitation simulated by 10 GCMs. *Climate Dyn.*, **19**, 383-395.

_____, K. Jin, K.-M. Lau, J. Shukla, V. Krishnamurthy, S. D. Schubert, D. E. Waliser, W. F. Stern, V. Satyan, A. Kitoh, G. A. Meeh, M. Kanamitsu, V. Y. Galin, J.-K. Kim, A. Sumi, G. Wu, and Y. Liu, 2002b: Intercomparison of GCM simulated anomalies associated with the 1997-98 El Niño. *J. Climate*, **15**, 2791-2805.

_____, J.-S. Kug, 2000: An El-Nino prediction system using an intermediate ocean and a statistical atmosphere, *Geophys. Res. Lett*., **27**(8), 1167-1170

_____, J.-Y. Lee, and C.-K. Park, 2004: Potential predictability of a dynamical seasonal prediction system with systematic error correction. *J. Climate*, **17**, 834-844.

Kirtman, B. and J. Shukla, 2002: Interactive coupled ensemble: A new coupling strategy for CGCMs. *Geophys. Res. Lett.*, **29**, 1367, doi: 10.1029/2002GL 014834.

Koster, R. D., and M. J. Suarez, 1992: Modeling the land surface boundary in climate models as a composite of independent vegetation stands. *J. Geophys. Res.*, **97**, 2697-2715.

Krishnamurti, T. N., C. M. Kishtawal, T. E. LaRow, D. R. Bachiochi, Z. Zhang, C. E. Willford, S. Gadgil, and S. Surendran, 1999: Improved weather and seasonal climate prediction forecasts from multimodel superensemble. Science, 285, 1548-1550.

_____, Kishtawal, C. M., Zhang, Zhan, LaRow, Timothy, Bachiochi, David, Williford, Eric, Gadgil, Sulochana, Surendran, Sajani, 2000 : Multimodel ensemble forecasts for weather and seasonal climate, *J. Climate*, **13**, 4196-4216

Kug, J.-S., I.-S. Kang, J.-Y. Lee, and J.-G. Jhun, 2004: A statistical approach to Indian Ocean sea surface temperature prediction using a dynamical ENSO prediction, *Geophys. Res. Lett.,* **31**, L09212, doi:10.1029/2003GL019209

Kumar, A., and M. P. Hoerling, 1995: Prospects and limitations of seasonal atmospheric GCM predictions. *Bull. Amer. Meteor. Soc*., 76, 335-345.

Kuo, H. L., 1974: Further Studies of the Parameterization of the Influence of Cumulus Convection on Large-Scale Flow. *J. Atmos. Sci*., **31**, 1232–1240.

Louis, J.F., M. Tiedtke, and J. F. Geleyn 1982: A short history of the operational PBL-parameterization at ECMWF, *Workshop on boundary layer parameterization*, *November 1981*, ECMWF, Reading, England.

Mellor, G. L., and T. Yamada, 1982: Development of a turbulence closure model for geophysical fluide problems. *Rev. Geophys. Space Phys.*, **20**, 851-875

Moorthi, S., and M. J. Suarez, 1992: Relaxed Arakawa-Schubert: A parameterization of moist convection for general circulation models. *Mon. Wea. Rev.* **120**, 978-1002.

Palmer, T. N., Alessandri, A., Andersen, U., Cantelaube, P., Davey, M., Délécluse, P., Déqué,, M., Díez, E., Doblas-Reyes, F. J., Feddersen, H., Graham, R., Gualdi, S., Guérémy, J.-F., Hagedorn, R., Hoshen, M., Keenlyside, N., Latif, M., Lazar, A., Maisonnave, E., Marletto, V., Morse, A. P., Orfila, B., Rogel, P., Terres, J.-M., Thomson, M. C.. 2004: Development of a european multimodel ensemble system for seasonal-to-interannual prediction (DEMETER). *Bull. Amer. Meteor. Soc*, **85**, 853–872.

Pan, H-L. and L. Mahrt, 1987: Interaction between soil hydrology and boundary layer developments. *Bound.-Layer Meteor*., **38**, 185-202.

Rowell, D. P., 1998: Assessing potential seasonal predictability with an ensemble of multidecadal GCM

simulations. *J. Climate*. **11**, 109-120.

_____, 1996: Reply to comments by Y. C. Sud and W. K.-M. Lau on Variability of summer rainfall over tropical North Africa (1906-92): Observations and modeling by D. P. Roweel, C. K. Folland, K. Maskell, and M. N. Ward (April 4, 1995, 121, 669-704): Futher analysis of simulated interdecadal North Africa. *Quart. J. Roy. Meteor. Soc*., **122**, 1007-1013.

_____, C. K. Folland, K. Maskell, and M. N. Ward, 1995: Variability of summer rainfall over tropical North Africa (1906-92): Observations and modeling. *Quart. J. Roy. Meteor. Soc*., **121**, 669-704.

Schubert, S., M. Suarez, C.-K. Park, and S. Moorthi, 1993: GCM Simulations of Intraseasonal Variability in the Pacific/North American Region. *J. Atmos. Sci.,* **50**, 1991–2007.

Sellers, P. J., Y. Mintz, Y. C. Sud, and A. Dalcher, 1986: A simple biosphere model (SiB) for use within general circulation model. *J. Atmos. Sci*., **43**, 505-531.

Shukla, J.,1975: Effect of Arabian Sea surface temperature anomaly on Indian summer monsoon: A numerical experiment with GFDL model. *J. Atmos. Sci.,* **32**, 503-511.

_____, 1981: Dynamical predictability of monthly means. *J. Atmos. Sci*., **38,** 2547-2572

_____, and B. M. Misra, 1977: Relationships between sea surface temperature and wind speed over the central Arabian sea and monsoon rainfall over India. *Mon. Wea. Rev.*, **105**, 998-1002.

Sperber, K. R., C. Brankovic, M. Deque, C. S. Frederiksen, R. Graham, A. Kitoh, C. Kobayashi, T. Palmer, K. Puri, W. Tennant, and E. Volodin, 2001: Dynamical seasonal predictability of the Asian summer monsoon. *Mon. Wea. Rev*., **129**, 2226-2247.

Stern, W., and K. Miyakoda, 1995: The feasibility of seasonal forecasts speculated from multiple GCM simulations. *J. Climate*, **8**, 1071-1085.

Waliser, D. E., Lau, K. M., Stern, W., Jones, C. 2003: Potential Predictability of the Madden–Julian Oscillation. *Bull. Meteorol. Soc*., **84**, 33–50.

Wang, B., I.-S. Kang, and J.-Y. Lee, 2004: Ensemble simulations of Asian-Australian monsoon variability during 1997/1998 El Nino by 11 AGCMs. *J. Climate*, **17**, 803-818

Ward, M. N., and A. Navarra, 1997: Pattern analysis of SST-forced variability in ensemble GCM simulations: Examples over Europe and the tropical Pacific. *J. Climate*., **10**, 2210-2220.

Webster, P.J., V.O. Magana, T. N. Palmer, J. Shukla, R.A. Tomas, M. Yanai and T. Yasunari, 1998: The monsoon: Processes, predictability and prediction. *J. Geophys. Res.*, **103**, 14451-14510.

Wu, Man Li C., Schubert, Siegfried, Kang, In-Sik, Waliser, Duane. 2002: Forced and Free Intraseasonal Variability over the South Asian Monsoon Region Simulated by 10 AGCMs. *J. Clim*. **15**, 2862–2880.

Xie, P., and P. A. Arkin, 1997: Global Precipitation: A 17-year monthly analysis based on gauge observation, satellite estimates and numerical model outputs. *Bull. Am. Meteor. Soc*., **78**, 2539-2558.

Yun, W. T., Stefanova, L., Krishnamurti, T. N., 2003 : Improvement of the multimodel superensemble technique for seasonal forecasts. *J.Climate*, **22**, 3834-3840

Zwiers, F. W., 1996: Interannual variability and predictability in an ensemble of AMIP climate simulations conducted with the CCC GCM2. *Climate Dyn*., **12**, 825-848.

Table 1. Description of the five models used in the present study.

Institute	Resolution	Physical parameterizations	
JMA	T63L40	Convection:	Prognostic Arakawa-Schubert scheme
		PBL:	Mellor-Yamada level-2 closure scheme
		Land sfc.:	Simple Biosphere Model (Sellers et al. 1986)
KMA	T106L21	Convection:	Kuo scheme (1974)
		PBL:	Meller and Yamada (1982) level 2 closure scheme
		Land sfc.:	Simple Biosphere Model (Sellers et al. 1986)
NASA	2^{o}x2.5^{o}L34	Convection:	Relaxed Arakawa-Schubert scheme (Moorthi and Suarez, 1992)
		PBL:	Louis et al (1982)
		Land sfc.:	Mosaic LSM (Koster and Suarez, 1992)
NCEP	T62L28	Convection:	Relaxed Arakawa-Schubert scheme (Moorthi and Suarez, 1992)
		PBL:	Non-local diffusion scheme (Hong and Pan, 1996)
		Land sfc.:	OSU two-layer model (Pan and Mahrt, 1987)
SNU	T63L21	Convection:	Relaxed Arakawa-Schubert scheme (Moorthi and Suarez, 1992)
		PBL:	Non-local diffusion (Holtslag and Boville, 1993)
		Land sfc.:	NCAR LSM (Bonan, 1995)

Table 2. Simple description of the 7 ocean-atmosphere coupled models used in a tier-one multi-model seasonal prediction system of DEMETER.

Institute	AGCM	Resolusion	OGCM	Resolution
CERFACS	ARPEGE	T63 31 Levels	OPA 8.2	2.0x2.0 31 Levels
ECMWF	IFS	T95 40 Levels	HOPE-E	1.4x0.3-1.4 29 Levels
INGV	ECHAM-4	T42 19 Levels	OPA 8.1	2.0x0.5-1.5 31 Levels
LODYC	IFS	T95 40 Levels	OPA 8.2	2.0x2.0 31 Levels
Meteo- France	ARPEGE	T63 31 Levels	OPA 8.0	182GPx152GP 31 Levels
Met Office	HadAM3	2.5x3.75 19 Levels	GloSea OGCM based on HadCM3	1.25x0.3-125 40 Levels
MPI	ECHAM-5	T42 19 Levels	MPI-OM1	2.5x0.5-2.5 23 Levels

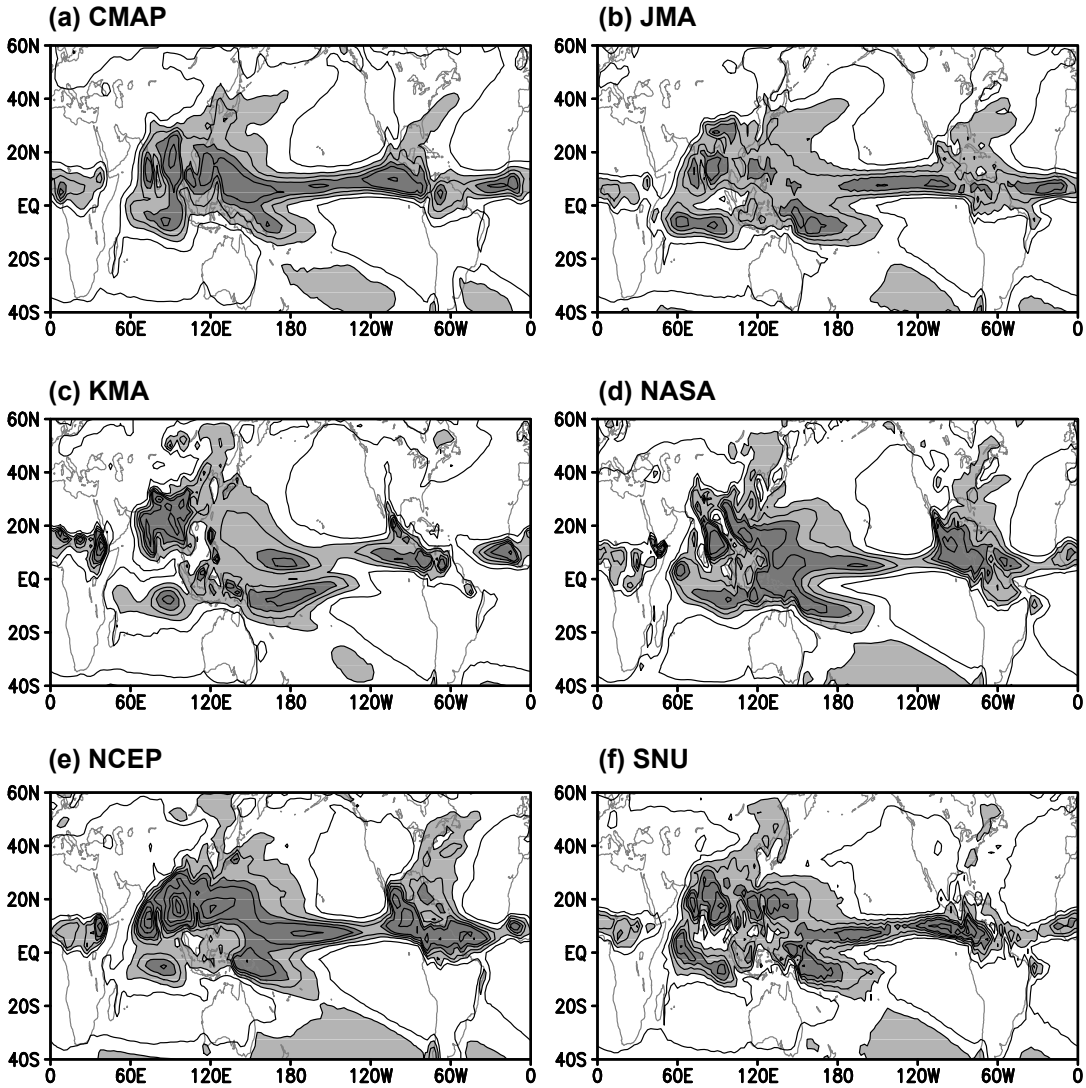

Fig. 1. Climatological summer mean precipitation. (a) Observation, (b)-(f), JMA, KMA, NASA, NCEP, and SNU models. Contour interval is 2, 4, 6, 8, 10, 15, 20, 25, and 30 mm/day and light and dark shadings indicate the rainfall rate more than 4 and 8 mm/day, respectively.

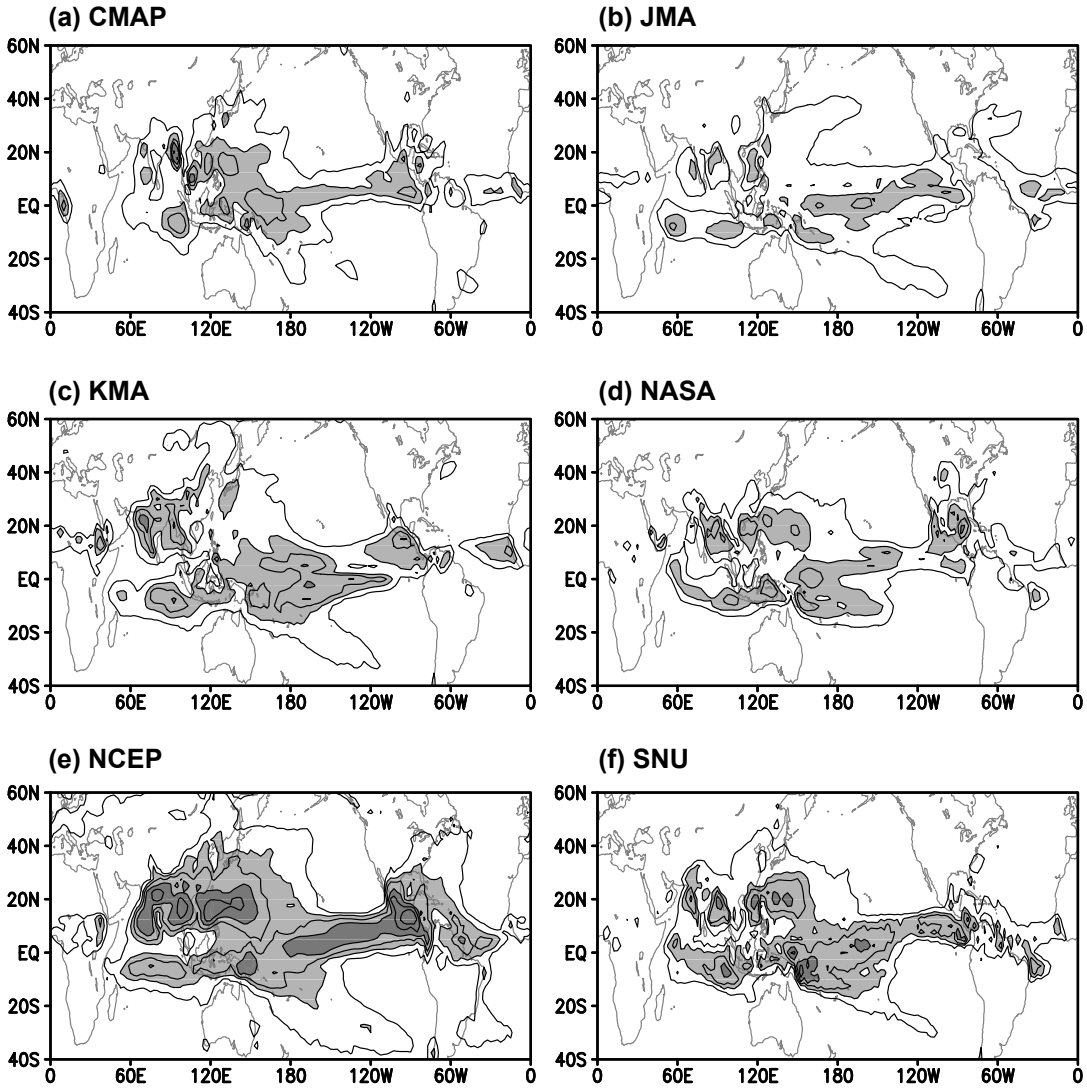

Fig. 2. Variances of summer mean precipitation anomalies for the 21years of 1979-1999. (a) CMAP observation precipitation, (b) JMA, (c) KMA, (d) NASA, (e) NCEP, and (f) SNU prediction models. Variance of each model is computed using all ensemble members of 21 year predictions. Contour interval is 1, 3, 6, 12, 24, and 48 mm^2/day^2 and light and dark shadings indicate the variance more than 3 and 12 mm^2/day^2, respectively.

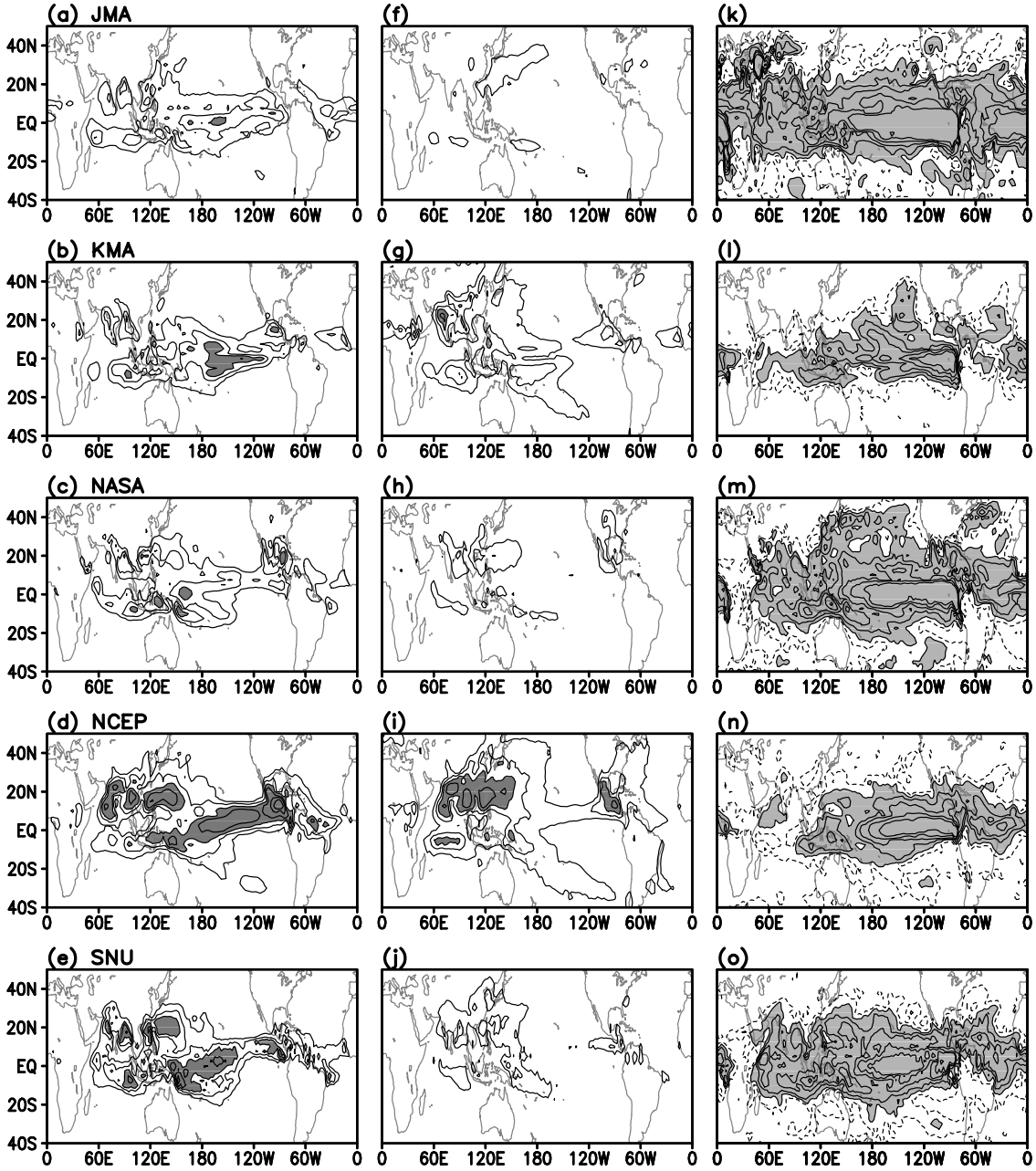

Fig. 3. (a)-(e) External variance of precipitation based on the ensemble average of each year. (f)-(j) Internal variance based on the deviation of individual members from the ensemble average. Contour interval is 1, 3, 6, 12, 24 and 36 mm^2/day^2 and shading indicates the variance more than 6 mm^2/day^2. (k)-(o) Signal to noise ratio defined by ratio of the forced variance to the free variance. Contour levels are 1, 2, 4, 8, and 16 and the dashed line indicates 0.5. Shading indicates the signal to noise ratio bigger than 1. Each model is marked at the upper-left corner of each panel.

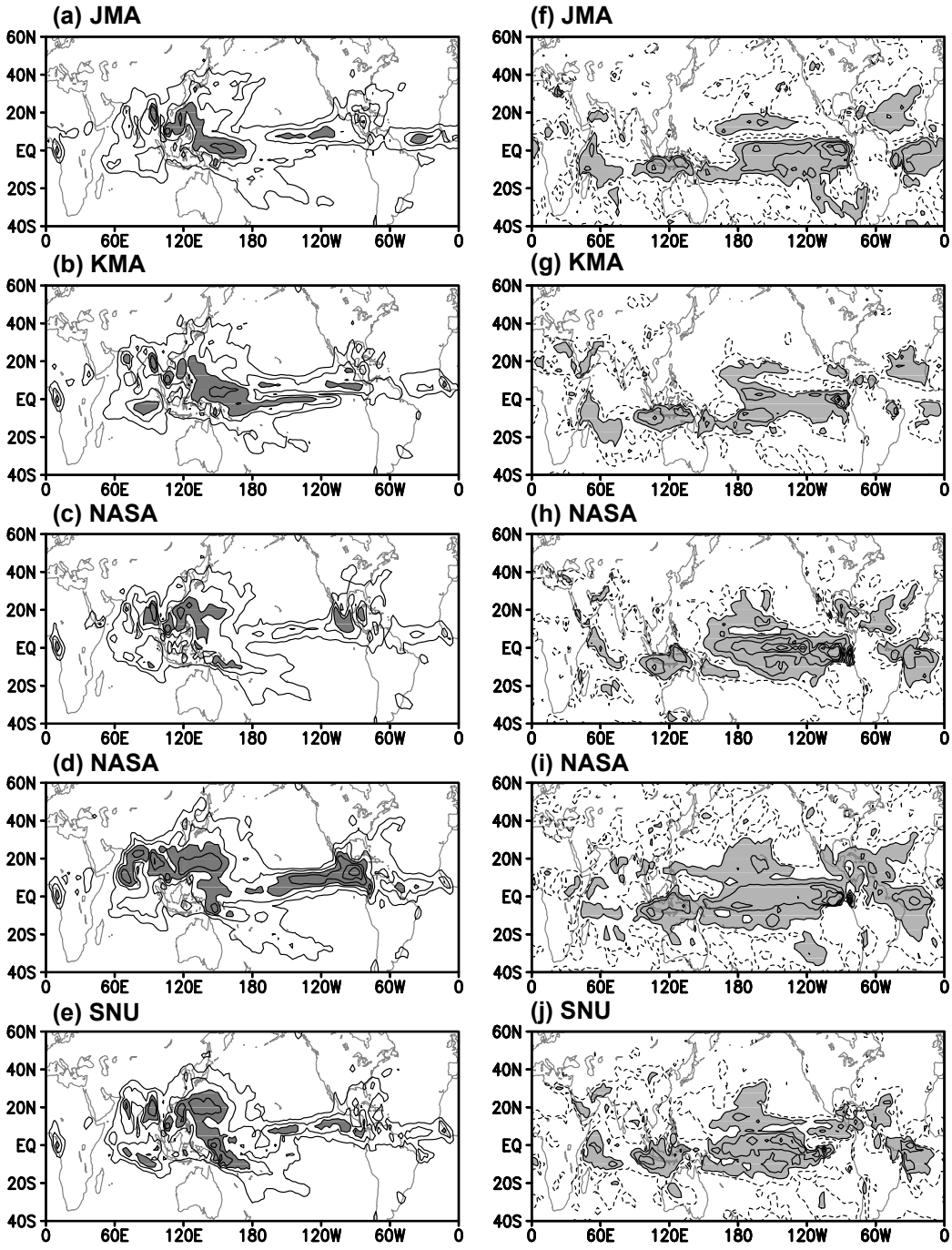

Fig. 4. (a)-(e) Variance of the systematic error, the difference between the ensemble average of prediction and the corresponding observation. Contour interval is 1, 3, 6, 12, 24, and 36 mm^2/day^2 and shading indicates the variance more than 6 mm^2/day^2. (f)-(j) Ratio between the variances of ensemble mean and systematic error. Contour levels are 1, 2, 4, and 8 and the dashed line indicates 0.5. Shadings indicates the ratio bigger than 1. Each model is marked at the upper-left corner of each panel.

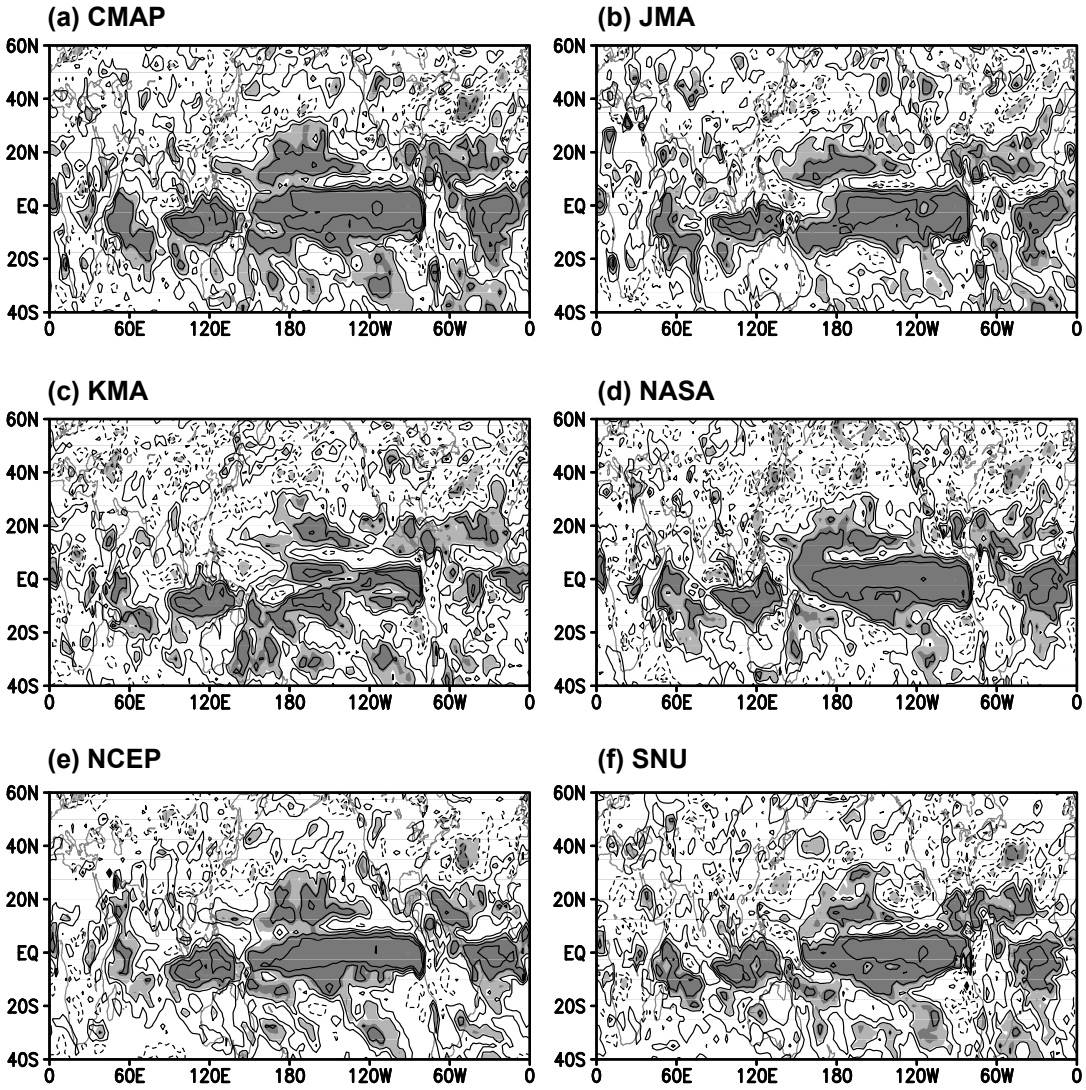

Fig. 5. Distribution of correlation coefficient between the observed and simulated ensemble-mean precipitation at each grid point. Each model case is marked at the upper-left corner of each panel, and the five model composite case is shown in (a). Contour interval is 0.2 and light and dark shadings denote the correlation coefficient significant at 95%(0.433) and 99%(0.549) confidence level, respectively. Zero line is not drawn.

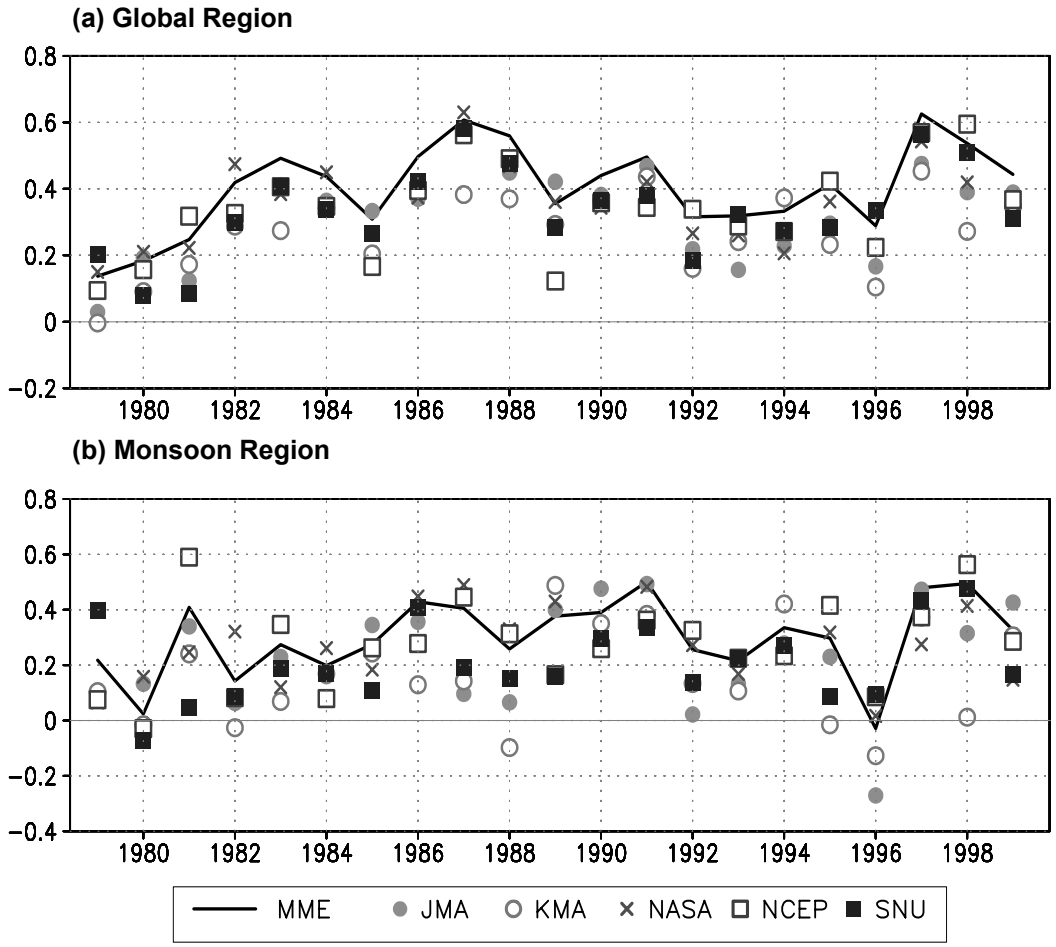

Fig. 6. Spatial pattern correlation coefficients between the observed and predicted ensemble-mean precipitations (a) over the globe (0-360^{O}E and 60^{O}S-60^{O}N) and (b) over the Monsoon region (40-160^{O}E and 20^{O}S-30^{O}N). Correlation values of each model and model composite are shown by various marks denoted in the figure.

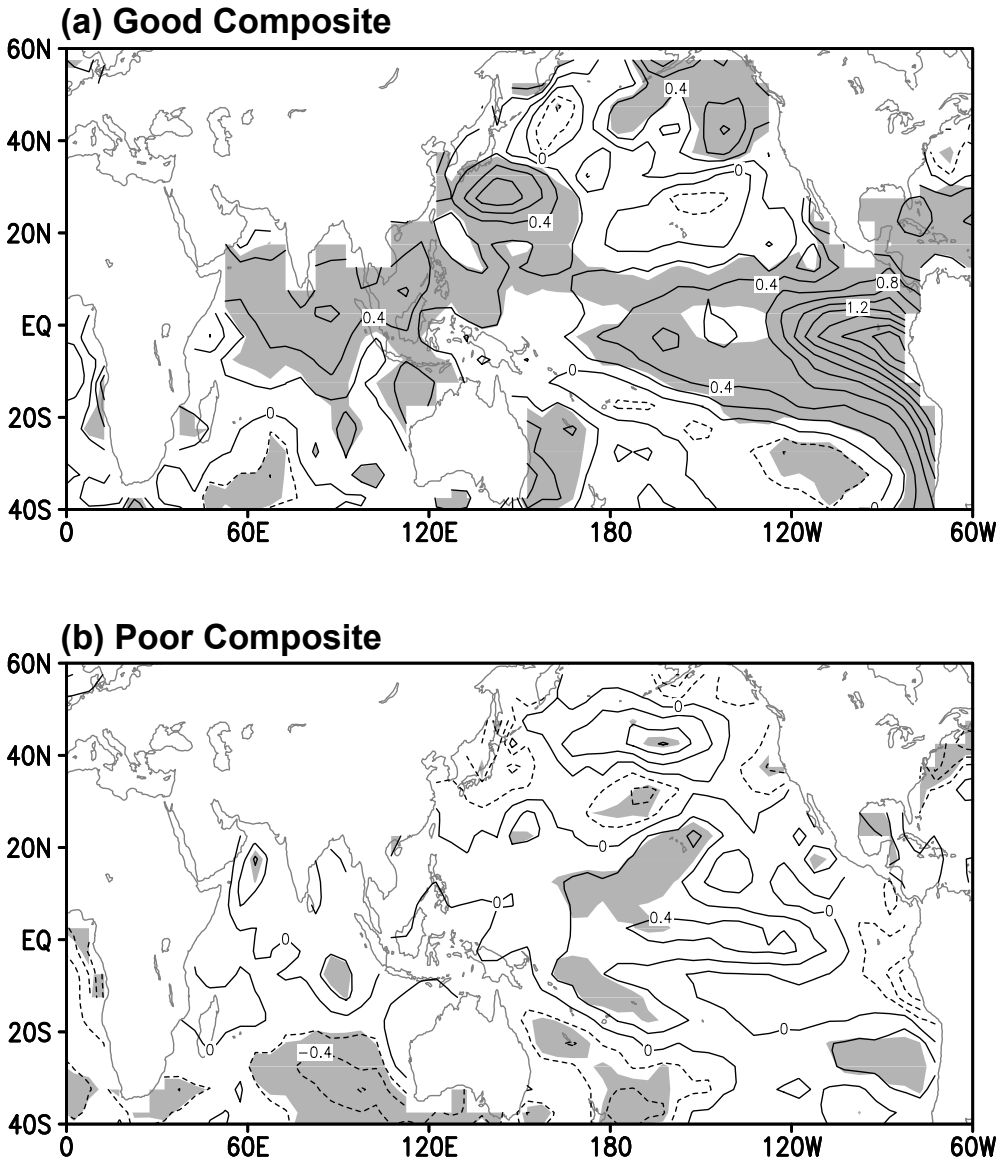

Fig. 7. (a) Composite SST anomalies for the years of good Monsoon prediction, 1991, 97, and 98. (b) Those for the years of poor Monsoon prediction, 1980, 82, 96. Selected cases exceed the one standard deviation of correlation coefficients. Shading denote the anomalies that are significant at the 99% level of each grid point (*Student t*-test).

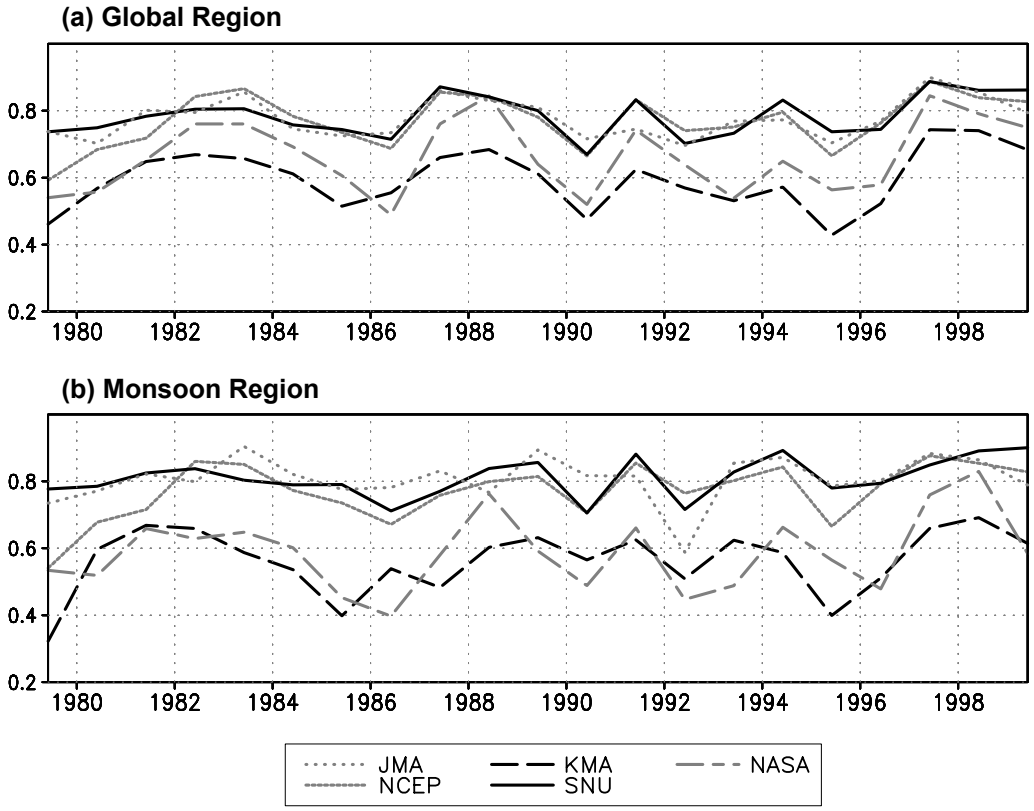

Fig. 8. Perfect model correlations of various models. (a) global spatial pattern correlation (0-360^{O}E and 60^{O}S-60^{O}N), and (b) the pattern correlation for the Monsoon region (40-160^{O}E and 20^{O}S-30^{O}N).

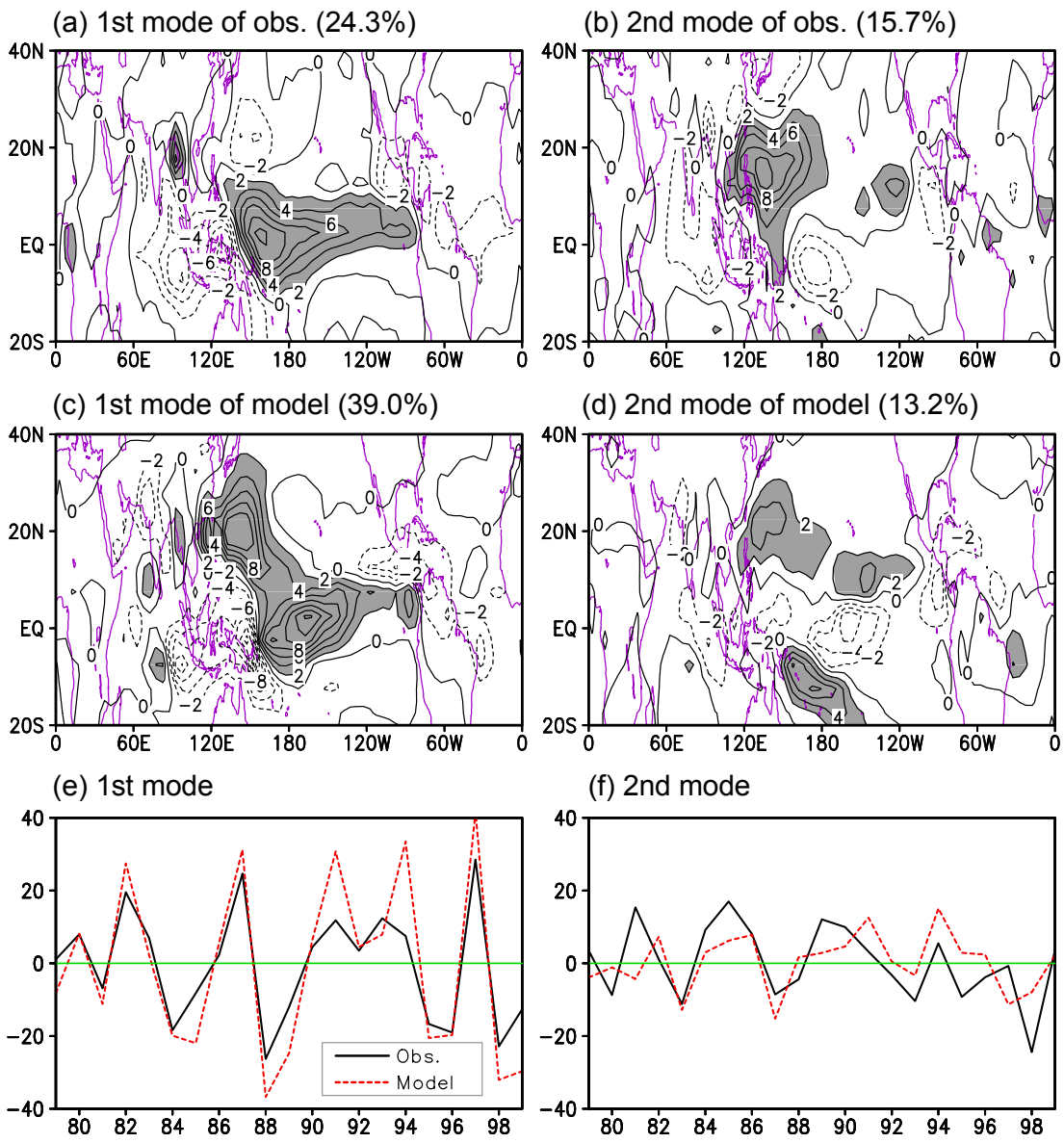

Fig. 9. EOF modes of the observed and simulated ensemble-mean precipitation. (a) and (b) are the observed first and second eigenvectors, (c) and (d) the simulated counter parts. (e) and (f) are the time series associated with the eigenvectors. Solid and dashed lines indicate the observed and simulated time series, respectively.

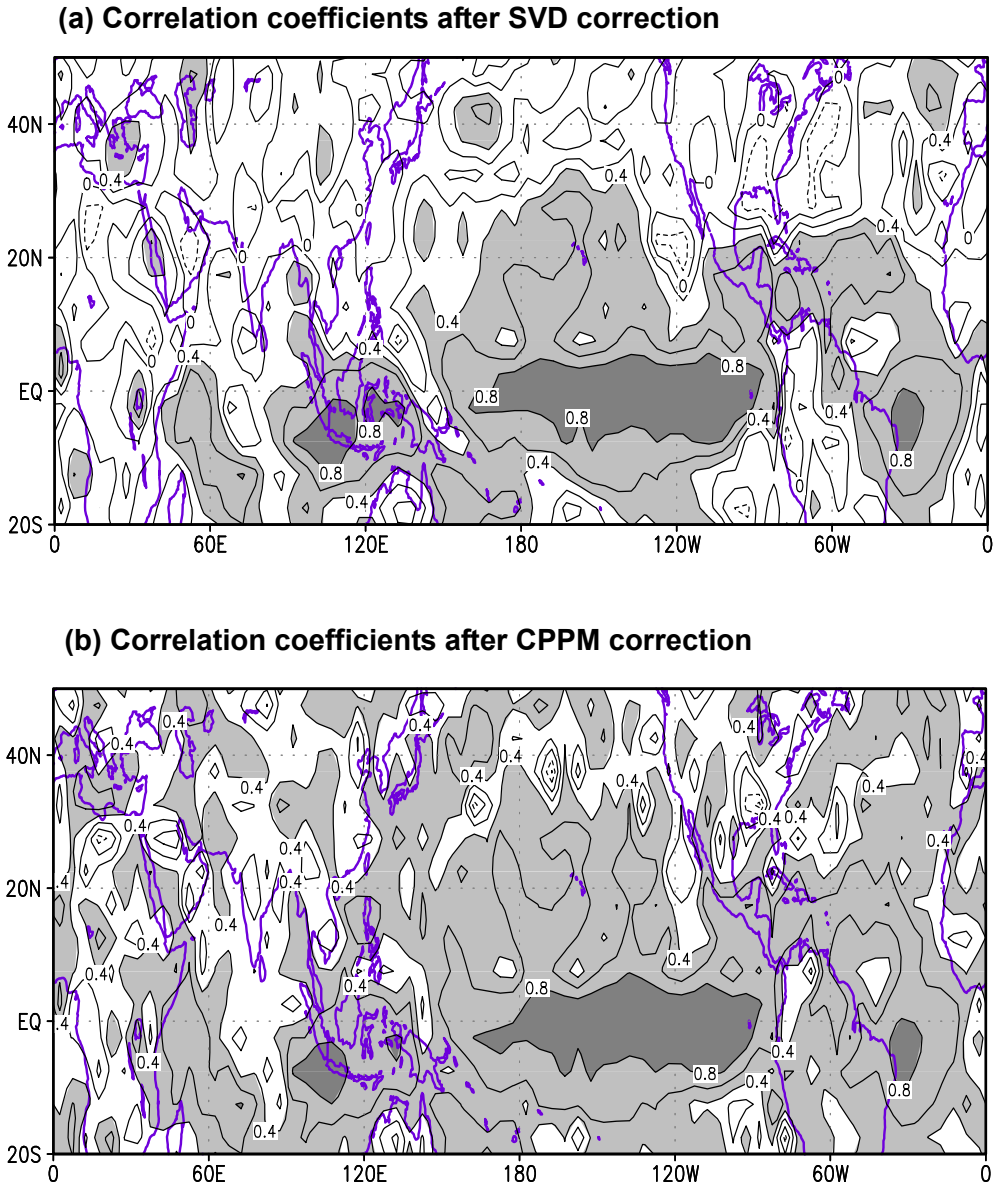

Fig. 10. As in Fig. 5 except the predicted precipitation of SNU SMIP after correction of systematic error using both (a) SVD and (b) CPPM.

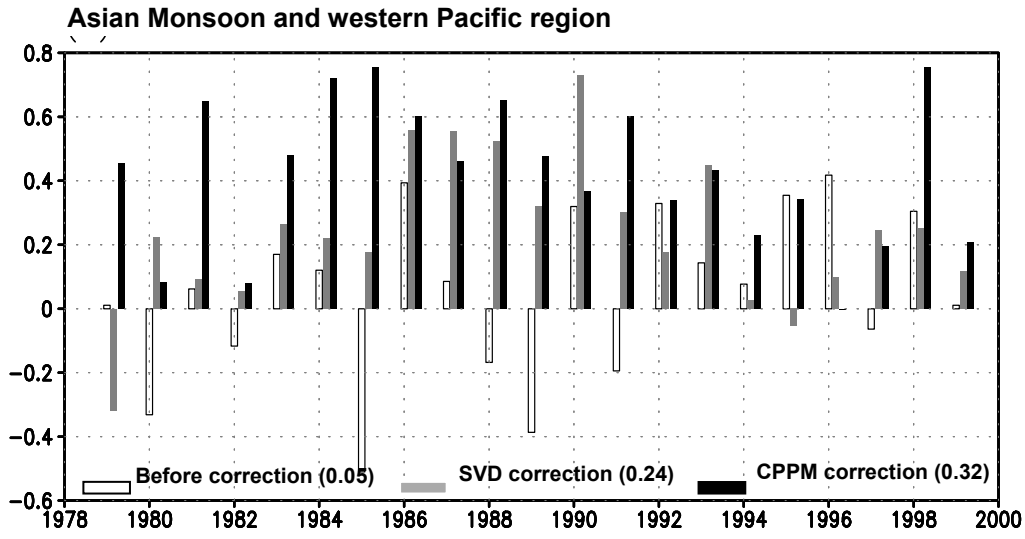

Fig. 11. Pattern correlation coefficients between the observed and predicted precipitations of SNU SMIP before (open bar) and after the bias correction by SVD (gray shaded bar) and CPPM (black shaded bar) over the Asian monsoon and western Pacific region (80-160^{O}E, 10-40^{O}N).

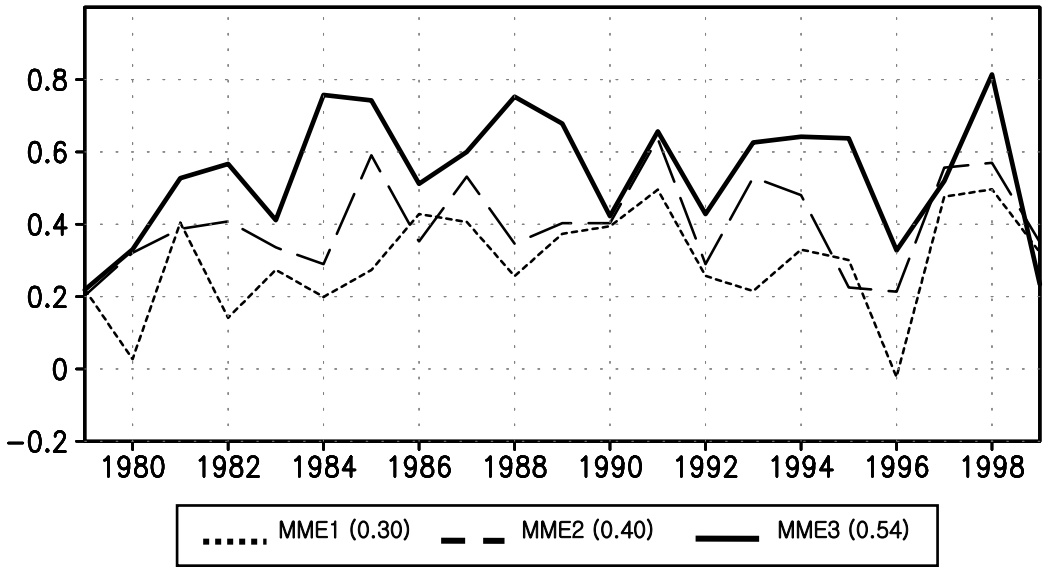

Fig. 12. Time series of spatial pattern correlations over the monsoon region (40 ^{O}E -160^{O}E and 20^{O}S-30^{O}N) between the observed and the predicted precipitations MME1 (dotted line), MME2 (dashed line), and MME3 (solid black line). MME1, MME2, and MME3 are the multi-model predictions based on a simple composite, SVD based superensemble, and the composite of correction predictions by CPPM, respectively.

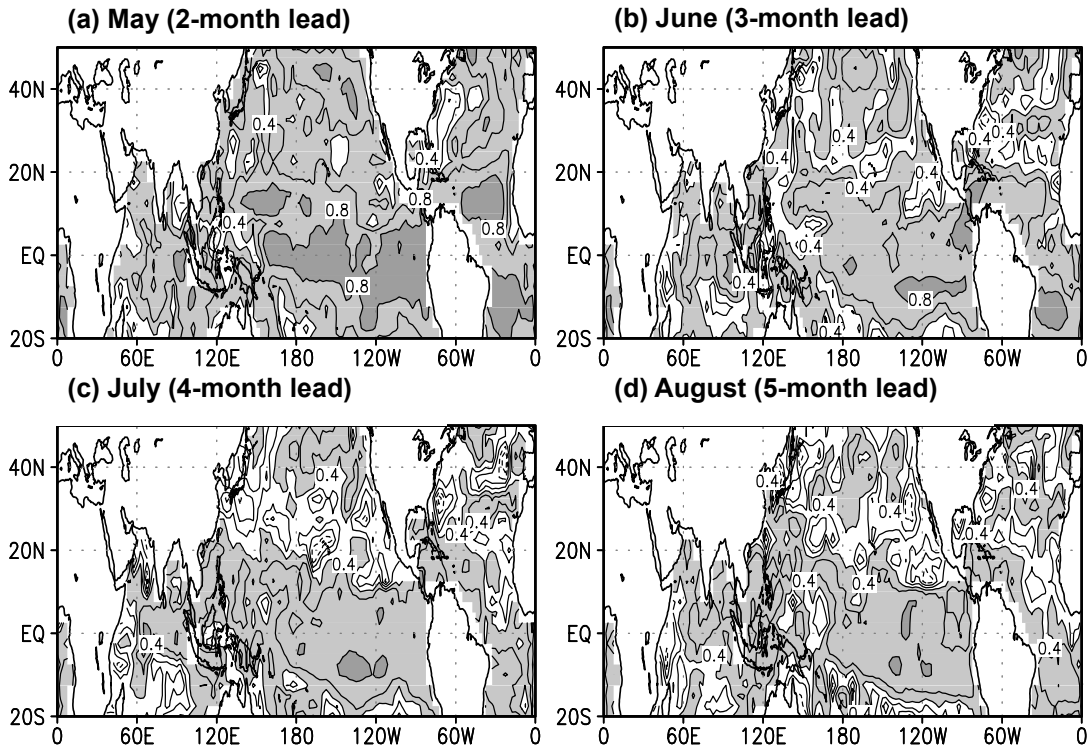

Fig. 13. Distribution of correlation coefficient between the observed and predicted summer-mean SST at each grid point for 21 years. The prediction data is from the SMIP/HFP of the SNU model.

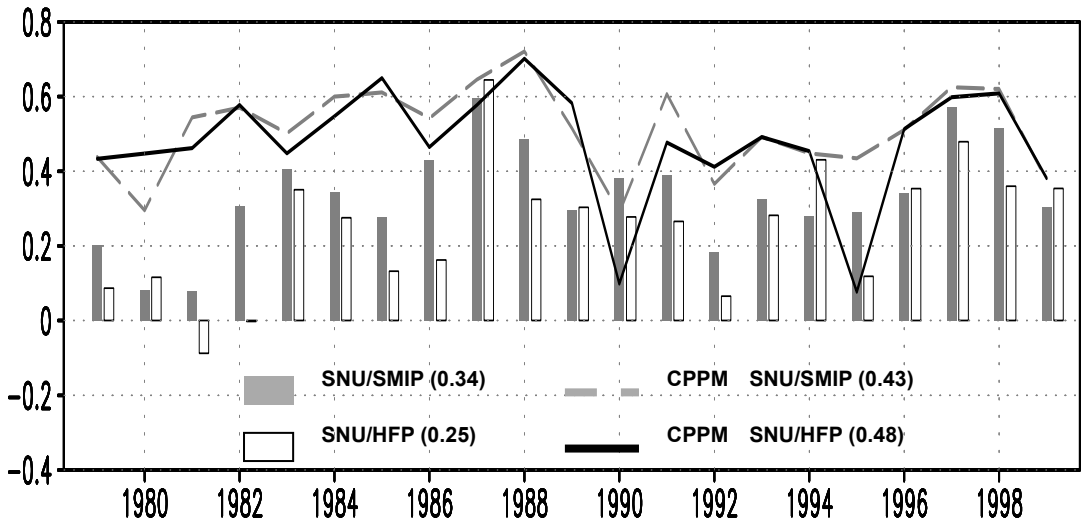

Fig. 14. Global Pattern correlation coefficient between the observed and predicted ensemble-mean precipitations. For the comparison, the correlation values for the SMIP and SMIP/HFP of the SNU model are shown by filled and open bars, respectively. The correlation values of the SMIP(gray) and SMIP/HFP(black) after statistical correction are shown by solid lines, respectively.

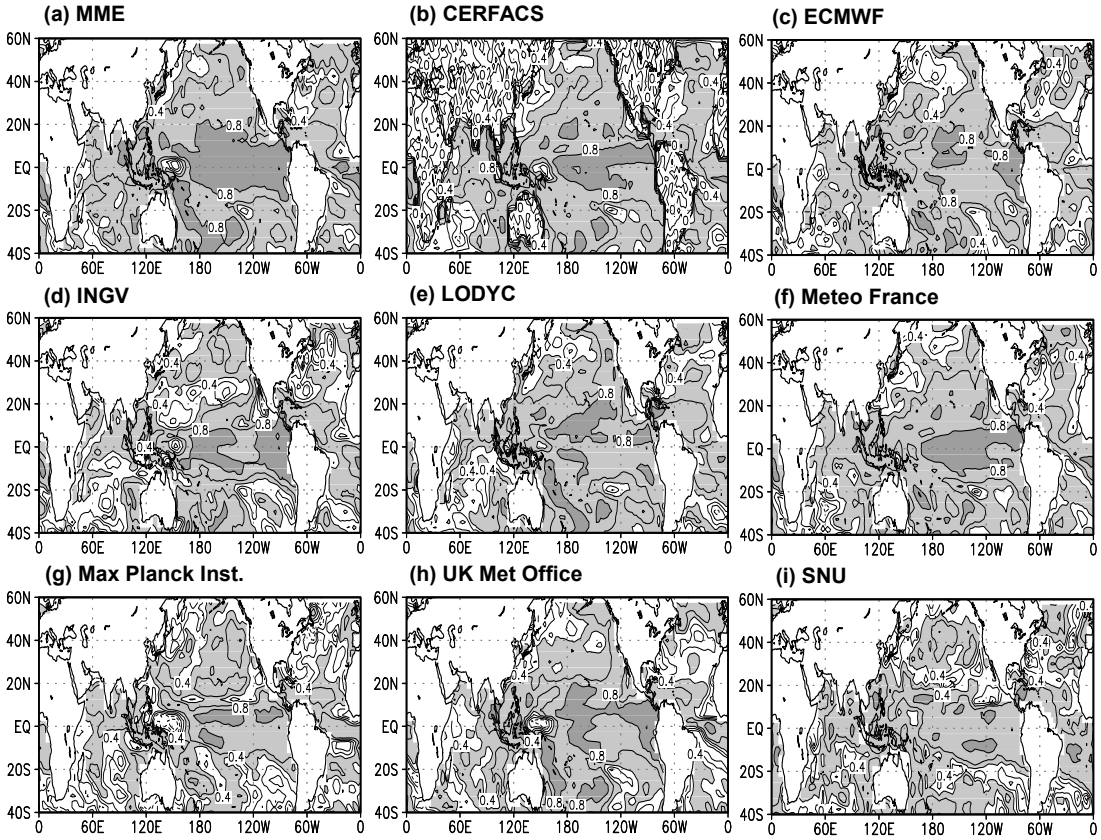

Fig. 15. Correlation coefficient of summer-mean SST for the multi-model ensemble (a) and the individual models (b-h) in a Tier-one system of DEMETER over the globe during 1980-1999. (i) is SST prediction skill of the SNU Tier-two system.

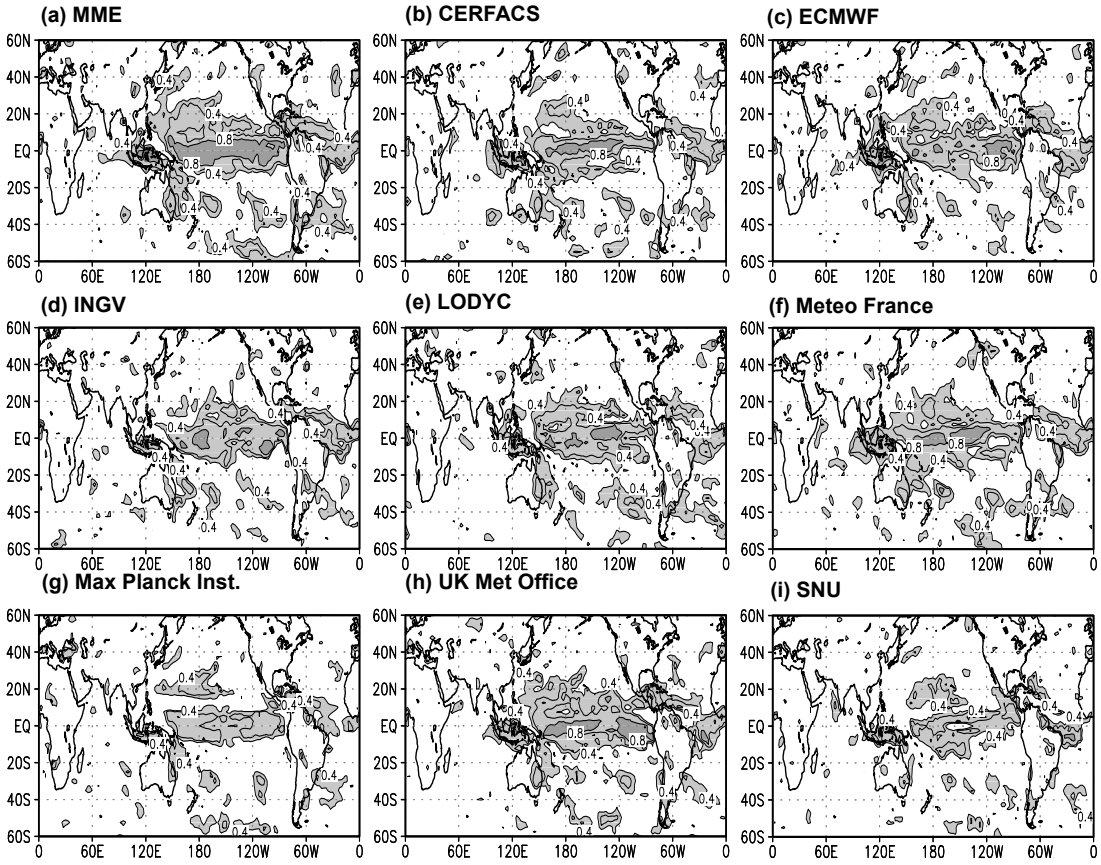

Fig. 16. Correlation coefficient of summer-mean precipitation for the multi-model ensemble (a) and the individual models (b-h) in a Tier-one system, DEMETER over the globe. (i) is the SNU Tier-two system.

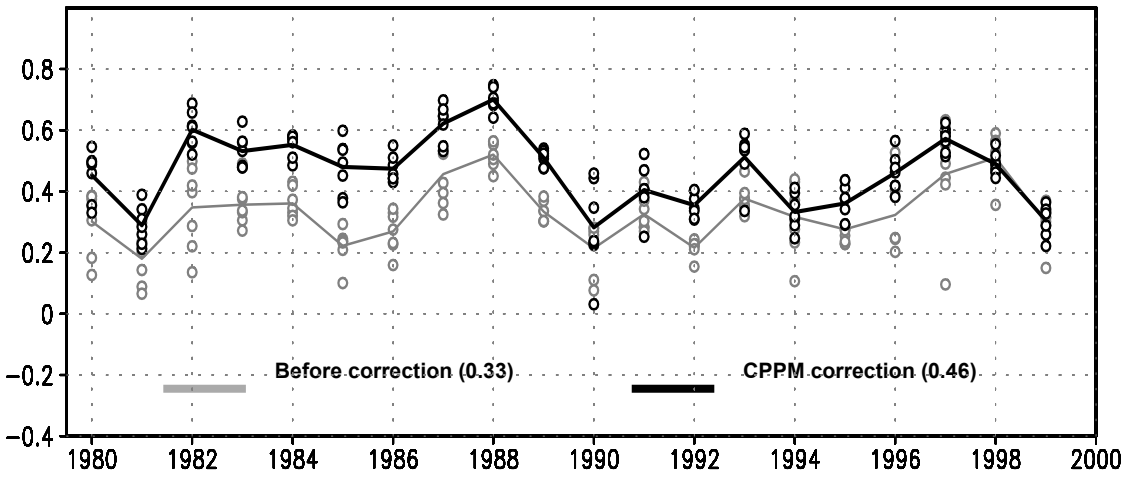

Fig. 17. The interannual variation of the averaged value of pattern correlation of the individual models before (gray) and after the bias correction (black) in a Tier-one system over the globe. The 20-year averaged correlation values are also written in caption as number.

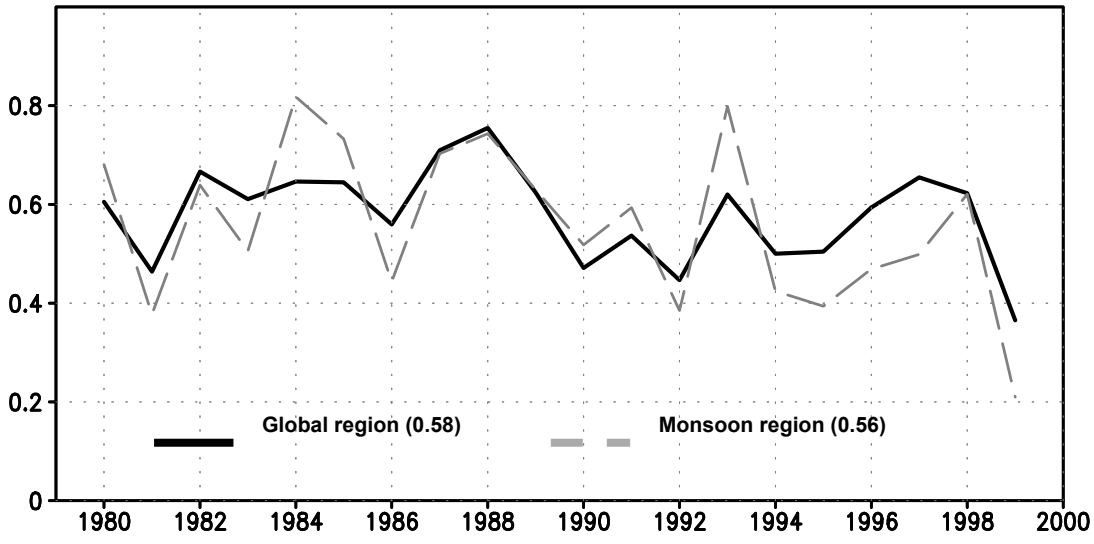

Fig. 18. Spatial pattern correlation between the predicted and observed precipitation over the global and monsoon region during 1980-1999. The correlation values of the composite after statistical correction of individual model in a Tier-one system (MME3) over the global and monsoon regions are written in caption.